

A NOVEL INJECTABLE POROUS HYDROGEL COMPOSITE SCAFFOLD FOR
BONE TISSUE ENGINEERING

by

PARVATHI NAIR

Presented to the Faculty of the Graduate School of
The University of Texas at Arlington in Partial Fulfillment
of the Requirements
for the Degree of

MASTER OF SCIENCE IN BIOMEDICAL ENGINEERING

THE UNIVERSITY OF TEXAS AT ARLINGTON

August 2010

Copyright © by PARVATHI NAIR 2010

All Rights Reserved

ACKNOWLEDGEMENTS

First, I thank my advisor Dr. Jian Yang, for giving me the opportunity to work in his lab. He showed me different ways to approach a research problem and the need to be persistent to accomplish any goal.

I would like to thank the rest of my thesis committee: Dr. Liping Tang and Dr. Harry Kim for sparing the time to be on my committee and having reviewed my work and provided valuable suggestions.

Let me also say thank you to the following people in the lab: Dipendra Gyawali, Richard Tran and Jagannath Dey for all the help they have given me in my project. They have always had the time to answer my questions and were very kind in giving me invaluable tips and suggestions. Also a big round of thanks to all my lab mates for all their help.

Last, but not least, I thank my family: my parents, Dr. R. Mohanchand, and Geetha Mohanchand, for encouraging and supporting me in every endeavor. Words are inadequate to express all that you mean to me. My brother Dr. Prakash Nair, for always being a patient listener, for always knowing the right thing to say to me when I am down and for always believing in me.

July 16, 2010

ABSTRACT

A NOVEL INJECTABLE POROUS HYDROGEL COMPOSITE SCAFFOLD FOR BONE TISSUE ENGINEERING

PARVATHI NAIR, M.S

The University of Texas at Arlington, 2010

Supervising Professor: Jian Yang

Over the past decade there has been an increasing use of bone grafts for orthopedic applications. With the aging US population, the need for suitable bone grafts substitutes has also increased. The long term goal of this study was to develop a novel in situ crosslinkable hydrogel composite for tissue-engineering critical-sized bone defects. This system consists of a newly developed water-soluble biodegradable hydrogel Poly ((ethylene glycol) maleate citrate) (PEGMC) [1] and hydroxyapatite (HA). The PEGMC/HA system is completely injectable and can be crosslinked in situ into crosslinked PEGMC/HA (CPEGMC/HA) hydrogel composite with or without poly (ethylene glycol) diacrylate (PEGDA) as a crosslinker. The hydrogel composite was found to have tunable mechanical properties and degradation profile that could be varied by adjusting the HA concentration and polymer compositions. CPEGMC/HA induced rapid and high degree of mineralization when incubated in vitro in simulated body fluid as quantified by SEM/EDX. In hydrated state the composite exhibited highly porous structures with the pore size ranging between 100- 400 μm . In vitro biocompatibility of the hydrogel composite system was tested against human fetal

osteoblast (hFOB1.19). The presence of pendant groups in the hydrogel network as confirmed by FTIR and ^1H NMR was used to covalently immobilize collagen on the surface to enhance cellular response. Osteoblasts (hFOB 1.19) showed good viability when seeded on the surface or encapsulated inside the polymer network as confirmed by LIVE/DEAD assay. The encapsulation of hFOB 1.19 inside the polymer network promoted cellular proliferation and activity as confirmed by DNA assay and the production of alkaline phosphatase (ALP) and calcium. In vitro cellular studies showed the composites to be a competent potential injectable vehicle for the transport of cells and other biomolecules such as desferrioxamine (DFO) which can aid in the regeneration of critical sized defects in bone.

TABLE OF CONTENTS

ACKNOWLEDGEMENTS	iii
ABSTRACT	iv
LIST OF FIGURES	ix
LIST OF TABLES	xi
LIST OF ABBREVIATIONS	xii
Chapter	Page
1. INTRODUCTION	1
1.1 Need for Bone Tissue Engineering	1
1.2 Current Available Treatments	1
1.3 Tissue Engineering Paradigm	2
1.4 Bone : Structure and Properties	3
1.5 Bone Tissue Engineering	4
1.5.1 Metallic Implants	5
1.5.2 Ceramics	6
1.5.3 Polymers	6
1.6 Citric Acid Based Polymers	8
1.7 Objectives of this Research	9
2. MATERIALS AND METHODS	10
2.1 Materials	10
2.2 Synthesis of PEGMC	10
2.3 Polymer Characterization	11
2.4 Preparation and Characterization of CPEGMC/HA	11

2.4.1	Sol Content	12
2.4.2	Swelling Ratio	12
2.4.3	Degradation Profile	13
2.4.4	Mechanical Properties	14
2.5	CPEGMC/HA Scaffold Pore Morphology	14
2.6	In Vitro Mineralization	15
2.7	Osteoblast Culture	15
2.8	Osteoblast Surface Seeding on CPEGMC/HA	16
2.9	Osteoblast Encapsulation	16
2.9.1	DNA Assay	17
2.9.2	ALP Activity Assay	17
2.9.3	Analysis of Calcium Content	18
2.10	Drug Release Study	18
2.11	Statistical Analysis	19
3.	RESULTS	20
3.1	Polymer Characterization	20
3.2	Preparation and Characterization of CPEGMC/HA	25
3.2.1	Sol Content	25
3.2.2	Swelling Ratio	27
3.2.3	Degradation Profile	28
3.2.4	Mechanical Properties	30
3.3	CPEGMC/HA Scaffold Pore Morphology	34
3.4	In Vitro Mineralization	36
3.5	Cellular Studies	38
3.5.1	Osteoblast Surface Seeding on CPEGMC/HA	38
3.5.2	Osteoblast Encapsulation	41

3.6 Drug Release Study	46
4. DISCUSSION	47
5. CONCLUSION	53
6. FUTURE RECOMMENDATIONS	54
REFERENCES	55
BIOGRAPHICAL STATEMENT	62

LIST OF FIGURES

Figure	Page	
3.1	Synthesis schematic of PEGMC. PEGMC prepolymer was synthesized by a simple polycondensation reaction using the monomers citric acid, PEG and maleic anhydride. Redox polymerization using APS/TEMED was used to fabricate the CPEGMC films. HA was added to the crosslinking solution to make CPEGMC/HA films	22
3.2	FT-IR spectra of PEGMC prepolymers	23
3.3	¹ H-NMR spectra of PEGMC 0.6	24
3.4	Sol content of CPEGMC/HA where PEGMC 0.6 was crosslinked with different HA concentration. Error bars represent standard deviations (n = 8). * corresponds to p < 0.05	26
3.5	Swelling ratio of CPEGMC/HA where PEGMC 0.6 was crosslinked with different HA concentrations. Error bars represent standard deviations (n = 8)	27
3.6	In vitro degradation of CPEGMC/HA where PEGMC 0.6 was crosslinked with different HA concentrations in PBS (pH 7.4; 37 °C). CPEGMC/HA was crosslinked using APS/TEMED redox initiators using PEG-DA 3400 as a crosslinker	29
3.7	Compressive modulus of non hydrated CPEGMC/HA where PEGMC 0.6 was crosslinked with different HA concentrations. * corresponds to p < 0.05 and # represents p < 0.01	31
3.8	Compressive mechanical strength of CPEGMC/HA when fully hydrated where PEGMC 0.6 is crosslinked with different HA concentrations. The CPEGMC/HA composites were immersed in DI-water till weight equilibrium was reached and then tested. * corresponds to p < 0.05 and # represents p < 0.01	32
3.9	Hysteresis of CPEGMC/HA films where PEGMC 0.6 was crosslinked with different HA concentrations. The samples were loaded to 20% strain and held for 30 seconds before the samples were unloaded	33
3.10	Characterization of pore morphology in CPEGMC scaffolds with different HA concentrations. Fig A), B), C) and D) shows micropho-	

tographs of CPEGMC 0.6, CPEGMC/HA (30), CPEGMC/HA (45) and CPEGMC/HA (60) when hydrated and cryosectioned to show the porous morphology	35
3.11 In vitro mineralization of CPEGMC/HA films when incubated in 5X SBF for 7 days. Fig A) and B) shows SEM image of the surface of CPEGMC 0.6 films when incubated in 5x SBF at day 1 and day 7 respectively. Fig C) and D) shows SEM image of the surface of CPEGMC/HA (45) when incubated in 5x SBF at day 1 and day 7 respectively. Fig C) and D) shows the entire surface of CPEGMC/HA covered with CaP minerals	37
3.12 FTIR spectra of CPEGMC 0.6 and collagen modified CPEGMC films	39
3.13 Fig A) CFDA-SE dye stained hFOB 1.19 seeded on CPEGMC/HA film after day 2 of subculture. Fig B) CFDA-SE dye stained collagen modified CPEGMC/HA surface seeded with hFOB 1.19 after day 2. Fig C) and D) SEM images of hFOB 1.19 surface seeded on CPEGMC/HA and collagen modified CPEGMC/HA surface respectively	40
3.14 Human fetal osteoblast hFOB 1.19 were encapsulated using redox polymerization in CPEGMC and CPEGMC/HA hydrogels. Viability was assessed using LIVE/DEAD assay. Live cells fluoresce green whereas dead cells fluoresce red. Fig A) cryostat section of CPEGMC/HA encapsulated with cells stained with H & E shows even distribution of cells in the polymer HA matrix. Fig B) SEM image of encapsulated cell. Fig C) and D) LIVE/DEAD stained CPEGMC/HA hydrogels at day 7 and day 21. Fig E) and F) LIVE/DEAD stained CPEGMC hydrogels at day 7 and day 21	42
3.15 DNA content of cell/polymer (CPEGMC and CPEGMC/HA) constructs at days 7, 14 and 21. Samples were performed in triplicate. * represents $p < 0.05$	43
3.16 ALP content of cell/polymer (CPEGMC and CPEGMC/HA) constructs at days 7, 14 and 21. Samples were performed in triplicate. * represents $p < 0.05$	44
3.17 Calcium content of cell/polymer (CPEGMC and CPEGMC/HA) constructs at days 7, 14 and 21. Samples were performed in triplicate. * represents $p < 0.05$	45
3.18 DFO drug release profile over time. Desferrioxamine was encapsulated in CPEGMC hydrogel and the release was measured over 7 days. Error bars represent standard deviation. ($n = 5$)	46

LIST OF TABLES

Table		Page
2.1	Chemical composition of 1x SBF as mentioned in Tas et.al	15
3.1	Feed ratios and actual molar composition of different PEGMCs where MA and CA denote Maleic Anhydride and Citric Acid respectively . .	23
3.2	Elemental analysis of CPEGMC and CPEGMC/HA films before and after incubation in 5X SBF at day 7	36

LIST OF ABBREVIATIONS

PEGMC	Poly(Ethylene Glycol Maleate Citrate)
HA	Hydroxylapatite
CPEGMC	Crosslinked Poly (Ethylene Glycol Maleate Citrate)
PLLA	Poly(L-Lactic Acid)
PGA	Poly(Glycolic Acid)
PLGA	Poly L-Lactic co-Glycolic Acid
PCL	Poly Caprolactone
CUPE	Crosslinked Urethane Doped Polyester
POMaC	Poly Octanediol Maleate Citrate
PEG	Poly Ethylene Glycol
PEG-DA	Poly Ethylene Glycol Diacrylate
FDA	Food and Drug Administration
SEM	Scanning Electron Microscope
FT-IR	Fourier Transform Infrared Spectroscopy
ATCC	American Type Cell Collections
FBS	Fetal Bovine Serum
DMEM	Dulbecco's Modified Eagle's Medium
hFOB 1.19	Human Fetal Osteoblast
ALP	Alkaline Phosphatase

CHAPTER 1

INTRODUCTION

1.1 Need for Bone Tissue Engineering

Bone has an inherent ability to repair itself and this regenerative ability is compromised when the defect is above a critical size [2]. There have been about 8 million cases of fracture reported annually in the US alone. Of these incidents, 5-10% resulted in non-union healing of the bone [3]. The estimated cost for treating these fractures has been projected at 5 billion dollars and as a result of non healing of critical size defects of bone, patient quality of life is affected [4].

1.2 Current Available Treatments

The current treatments for non healing bone fractures include autografts, allografts and metallic prosthetic implants. Autografts are the gold standard in bone defect treatment. They are harvested from the patient's iliac crest and transplanted in the bone defect. Autografts assists in the natural bone remodeling process resulting in critical size defect repair. Autografts require the patient to undergo two very invasive surgeries. The first procedure is done to harvest the graft and the second surgery is performed to transplant the harvested graft. As a result the possibility of infection is very high and the post operative recovery is long and painful. In addition, autografts are not easily available. The limited number and quality of grafts can affect the bone regeneration. Allografts are commonly used in the treatment of bone defects. Allograft bone is obtained from a donor and matched to a recipient. unlike

autograft, allograft is an avascular and non-viable tissue. Since they are absent of any osteoclast and osteoblast cells, they are deficient in bone remodeling. This results in a mismatch in weight loading resulting in microfractures and eventual failure of the graft. Since they are transplanted from one individual to another, there is always a chance of graft rejection by the recipient's immune system and disease transmission. The failure rate of allografts is as high as 25-35% [5]. Therefore, there exists the need for alternative paradigms to treat critical size defects which addresses the shortcomings of the above mentioned methods of treatment.

1.3 Tissue Engineering Paradigm

Tissue engineering involves the interaction of materials and cells to regenerate damaged tissue. One approach involves harvesting the patient's own cells and grow them in a controlled culture environment on a three dimensional scaffold. The construct when ready is delivered to the desired site in the patient's body. As new tissue regeneration takes place the scaffold will gradually degrade. Another approach involves the implantation of a scaffold to the desired site so as to direct tissue formation in situ. The human body is a highly complex system. The requirements that scaffold material needs to fulfill are varied and complex. Therefore the design and selection of the scaffold material is one of the primary concerns of tissue engineering. First, the material has to be biocompatible. The material when implanted inside the body must not cause an adverse and prolonged inflammatory response. Further the material must not be cytotoxic or cause an immunogenic reaction. Secondly, the scaffold must be biodegradable. On degradation, the byproducts must be non toxic to the body and must be cleared from the body through natural methods. In addition, scaffold material must have mechanical properties that are comparable to the target

tissue being replaced. The scaffold material must be able to handle the wear and tear of the implantation procedure and must not fail as the tissue regeneration takes place. Also, scaffold material before implantation must be sterilizable to prevent infection [6, 7].

Tissue engineering also must address the issue of material cell interaction. The ability of cells to proliferate and differentiate is determined by the interaction of cells and the underlying biomaterial. The biomaterial should provide a favorable environment for the cells to grow. Biofunctionalization of molecules such as peptides etc enhance cellular activity is an advantage. The physicochemical characteristics of the material such as hydrophobicity, charge and pH affects the cell viability [8].

Other key considerations involve the degree of porosity, pore size and extent of pore interconnectivity. Since the scaffold serves as a framework for cellular growth there exists the need for a high degree of scaffold porosity so that the cellular growth can result in penetration of cells inside the scaffold. The selection of cell type will determine the pore size of the resulting scaffold. The method of scaffold fabrication will influences the nature of the scaffold network. A biodegradable and biocompatible scaffold with a high degree of interconnected pores with suitable mechanical properties is the basic requirement for tissue engineering [9].

Tissue engineering design paradigms are unique for the target tissue. Therefore understanding the properties of natural bone is essential for designing a synthetic prosthetic that can closely mimic the function and property of native bone.

1.4 Bone : Structure and Properties

Bone is a highly vascularized and complex organ composed by weight of 60% inorganic minerals, 10% water and remaining part being made up predominantly of

type I collagen. The composition and interaction of all the constituent elements decides the function and properties of bone. Further classification of bone can be done based on architecture. (1)Cancellous bone and (2)Cortical bone. Compact bone is rigid and found mainly in the middle shaft of long bones and inside other bones. Cortical bone also known as the spongy bone is a highly porous structure which is filled with bone marrow [10].

The mechanical properties of natural bone are anisotropic, i.e. the strength of the bone depends on the orientation of the applied load. The various mechanical properties of cortical bone have been studied and are reported to vary greatly from a few hundred MPa to GPa. However due to the higher porous nature of the cancellous region of the bone, reported in the region of 70-95% porosity have been reported to be in the range of a few MPa to a few hundred MPa [11].

1.5 Bone Tissue Engineering

Understanding the structural, physical, chemical, biological and cellular properties of natural bone is imperative to designing a new approach that will deal with not only the basic tenets of tissue engineering but also address the unique challenges of designing a synthetic bone. In addition to specific functions depending on the location and nature of the bone in vivo, there are some requirements that tissue engineered bone must fulfill [10, 12].

1)Induce angiogenesis: Bone is highly vascular. Current failure in bone regeneration is due to the failure in inducing a high level of vasculature [9, 8].

2)Promote osteoconductivity: 60%of natural bone is composed of inorganic calcium phosphate minerals called dahllite [11]. To bridge the gap between non union and non healing bone, the implanted scaffold must have the ability to induce miner-

alization, i.e. be osteoconductive.

3) Promote osteoinductivity: The ability to cause non bone like cells to differentiate and form new bone is called osteoinductivity [13]. An osteoinductive material should therefore promote new bone formation in a location where the body cannot naturally heal on its own [14].

Depending on the chemical composition, bone graft substitutes can be classified into four different groups.

- 1) Metallic Implants such as titanium and its alloys, stainless steel etc.
- 2) Ceramic implants like bioactive glass, hydroxylapatite(HA), calcium phosphate etc.
- 3) Polymers
 - 3.1) Non biodegradable polymers like poly(methyl methacrylate), ultra high molecular weight polyethylene (UHMWPE).
 - 3.2) Biodegradable polymers which can be classified as natural polymers and synthetic polymers. Natural polymers include polysaccharides such as chitosan, hyaluronic acid derivatives etc) and proteins like collagen etc. Synthetic polymers such as poly lactic acid (PLA) , poly glycolic acid (PGA), poly caprolactone (PCL) etc [15].
- 4) Combination of ceramics with metals and polymers.

1.5.1 Metallic Implants

Metallic implants using titanium and its alloys and stainless steel have been widely used in load bearing orthopedic applications. They have shown to be fairly successful. However metallic implants are invasive and require surgeries to implant the device. Also, since they are neither biodegradable, osteoconductive, nor osteoinductive, there is no possibility of natural bone regrowth. Over time they fail due to problems associated with stress shielding, fatigue and loosening of implant. As a

result this line of treatment is not the most advantageous [16, 17].

1.5.2 Ceramics

Ceramics such as bioactive glass and calcium phosphates are an important category of materials for bone tissue engineering. Natural bone is made up of 60%wt of HA $Ca_{10}((PO_4)_6)(OH)_2$. Calcium phosphates have similar chemical and crystalline characteristics to bone mineral. Since they are inorganic minerals lacking any proteins they elicit minimal immune response. Thus, they have been shown to be biocompatible. Calcium phosphates surfaces cause an active layer of hydroxy carbonate apatite (HCA) to be formed in vivo. This biologically active layer is instrumental in tissue integration by providing a bonding interface between the material and the tissue. HCA phase is chemically and structurally similar to the mineral phase in bone. Thus calcium phosphates promote osteoconductivity. Calcium phosphates also promote osteoblast attachment, proliferation and differentiation with hydroxylapatite (HA) being the most effective. However if used alone, calcium phosphates have poor mechanical properties resulting in implant failure. Also the rate of degradation is very slow [14].

1.5.3 Polymers

1.5.3.1 Natural Polymers

Natural polymers such as chitosan, alginate, hyaluronic acid derivatives, collagen and cellulose have been used as scaffold materials in tissue engineering. Properties such as biodegradability and biocompatibility have made these materials attractive.

The ability of these materials to be crosslinked in vivo confers an additional advantage. However due to their poor mechanical properties and batch wise variations, large scale use of natural polymers is not feasible [18].

1.5.3.2 Synthetic Polymers

Synthetic polymers have also been explored extensively for bone tissue engineering applications. Prefabricated scaffold matrices using PLA, PGA, PLGA and PCL in combination with calcium phosphate have been studied. However these materials do not match the mechanical properties of the biological tissue as they are stiff and non compliant [19, 20, 21].

1.5.3.3 Injectable Polymers

Some of the recent work has focused on injectable in situ crosslinkable biodegradable materials. These materials have been extensively investigated as carriers of cells, drugs and other growth factors. These materials also have been used to bridge gaps and fill bone defects. Since these materials can conform to the shape of the cavity they are injected into, the need to fabricate scaffolds of any specific dimension is avoided. Also due to the injectable nature of the material, it is possible to deliver the polymer matrix in a minimally invasive procedure in hard to reach areas of the body thereby achieving a localized application of the polymer construct [22, 23, 24, 25].

1.6 Citric Acid Based Polymers

The currently FDA approved biomaterials are polylactones like poly(L-lactide) (PLA), poly(glycolide)(PGA) and their copolymers (PLGA). These biomaterials have shown excellent biocompatibility, but are stiff, inelastic and non compliant. The compliance mismatch between implant and scaffold leads to inflammation and scar tissue formation which prevents the integration of the implant with the surrounding tissue and also results in fatigue and stress shielding. Therefore, for soft tissue and load bearing applications, their use as scaffolding material is not ideal [26, 27]. Citric acid based biomaterials such as poly octanediol citrate (POC),crosslinked urethane doped polyester(CUPE),poly (octanediol maleate citrate)(POMaC) and poly((ethylene glycol) maleate citrate)(PEGMC) have been synthesized [26, 27, 28, 29]. These polymers are synthesized with easily available non toxic monomers. The synthesis is conducted through a simple polycondensation reaction. The resulting polymer is degradable through the ester bonds and the degraded products are non toxic. Citric acid, which is one of the key monomers is a byproduct of the kreb's cycle and also provides additional pendant groups for biofunctionalization post polymerization.

The advantages of an injectable system for bone tissue engineering are many. Hydrogels, are three dimensional networks that can uptake large amounts of water. They show excellent biocompatibility as they mimic physical characteristics similar to that of extracellular matrix. They are permeable, allowing the easy exchange of gases and other soluble metabolites and nutrients [30]. However this also makes them soft, elastic and mechanically weak. Many PEG based hydrogels have been investigated for use to treat bone defects. Mikos et al. have developed a biodegradable and injectable hydrogel system by reacting fumaric acid and polyethylene glycol (PEG) to synthesize a new oligomer,oligo[poly(ethylene glycol)fumarate](OPF). OPF was crosslinked using redox initiators in the presence of the crosslinker polyethylene gly-

col diacrylate (PEG-DA). OPF has been investigated as scaffolds and cell carriers for bone tissue engineering [23, 31, 32]. But PEG based hydrogels similar to OPF have weak mechanical strength and slow degradation profiles. Recently developed PEG based hydrogels such as poly(glycerolco-sebacate) acrylate (PGSA), poly(propylene fumarate)(PPF) and PEG sebacate diacrylate (PEGSDA) have enhanced mechanical strength and reduced degradation rates. Another hydrogel that has been investigated as an injectable bone cement is poly(propylene fumarate)(PPF). PPF was found to have tunable mechanical and degradation properties based on the degree of crosslinks and double bond in the crosslinked network [33].

Therefore we have developed a new citric acid based in situ crosslinkable polymer which provides the additional pendant groups for bioconjugation. In this synthesis, citric acid is reacted with maleic anhydride and poly ethylene glycol (PEG) in a simple polycondensation reaction to produce poly((ethylene glycol) maleate citrate)(PEGMC). The resultant polymer is water soluble and can be crosslinked using redox initiators in the presence or absence of a crosslinker. To improve strength, mineralization ability and osteoblast attachment and proliferation, PEGMC is combined with hydroxylapatite (HA) to make a polymer composite that can be crosslinked in situ (CPEGMC/HA).

1.7 Objectives of this Research

Aim 1: The aim of this project is to develop an injectable, in situ crosslinkable hydrogel composite with tunable mechanical and degradation properties.

Aim 2: To evaluate the injectable system as a competent cell and drug (DFO) delivery model.

CHAPTER 2

MATERIALS AND METHODS

2.1 Materials

All chemicals, cell culture medium and supplements were purchased from Sigma-Aldrich (St.Louise, MO) except where mentioned otherwise. All chemicals were used as received.

2.2 Synthesis of PEGMC

PEGMC was synthesized by a simple polycondensation reaction. Poly(ethylene glycol) (PEG) ($M_w=200$), citric acid and maleic anhydride were added to a 250 ml round bottom flask fitted with an inlet outlet adapter. The flask was immersed in silicon oil bath and melted at 160° C for 10 minutes at constant stirring of 360 rpm under continuous flow of nitrogen. Following the melting of the monomers, the temperature of the oil bath was reduced to 140°C for the remainder of the reaction. The stirring speed was reduced gradually to 100 rpm as the desired viscosity was achieved, the reaction was stopped and the prepolymer was dissolved in deionized water. The prepolymer was then filled into dialysis tube membrane with a molecular weight cut off of 500 Da and dialyzed for 2 days with constant change of water. This was done to leach out the low molecular weight oligomers and unreacted monomers. After dialysis, the prepolymer was freeze dried to get the final PEGMC.

To synthesize different PEGMC prepolymers, the molar ratio of maleic anhydride to citric acid (0.4:0.6, 0.6:0.4, 0.8:0.2) was changed to yield PEGMC 0.4, PEGMC 0.6 and PEGMC 0.8 respectively. The molar ratio of diol to acid was always kept

as 1:1. The molecular weight of the resultant prepolymer was characterized using an Autoflex Maldi-TOF spectrometer (Bruker Daltonics, Manning Park, MA).

2.3 Polymer Characterization

Fourier transform infrared (FT-IR) spectra of the PEGMC prepolymer were characterized using Nicolet 6700 FT-IR spectrometer (Thermo Fisher Scientific) equipped with OMNIC software at room temperature. The PEGMC prepolymers were dissolved in 1,4-dioxane to make a 5% w/v solution and cast on potassium bromide (KBr) crystals and allowed to dry. ^1H (Proton Nuclear Magnetic Resonance) spectra was recorded using MHz JNM ECS 300(JEOL, Tokyo, Japan) at ambient temperature to confirm the chemical structure of the prepolymer. Polymer solutions for NMR were prepared by making a 5%(w/v) solution in deuterated dimethyl sulfoxide-d6 (DMSO-d6) and the chemical spectra had tetramethylsilane (TMS) as the internal standard.

2.4 Preparation and Characterization of CPEGMC/HA

Redox crosslinked CPEGMC/HA networks were formed through radical polymerization. PEGMC prepolymer was dissolved in deionized water (DI-water) to make a 30% (w/v) solution. The solution was then neutralized by adding sodium bicarbonate to make the pH~(6-7). To this polymer solution polyethylene glycol diacrylate (PEG-DA, $M_w = 3400$ Da) added as a crosslinker.

To fabricate different crosslinked hydrogel composites, the weight ratio of PEGMC 0.6 to HA (70:30, 45:55, 30:70) was changed to yield CPEGMC/HA (30), CPEGMC/HA

(45) and CPEGMC/HA (60) respectively. Ammonium persulfate/*N,N,N',N'*-tetramethyl-ethane-1,2-diamine (APS/TEMED) was used to crosslink the prepolymer-HA solution using redox crosslinking. After the addition of the redox initiators the PEGMC/HA solution was tightly sealed and placed in 37 °C incubator till the prepolymer solution crosslinked completely to crosslinked PEGMC/HA (CPEGMC/HA).

2.4.1 Sol Content

CPEGMC/HA composites with different HA composition were made as previously described. The CPEGMC/HA samples were cut into circular discs of dimensions 10 mm diameter by 2 mm thickness ($n = 8$). The samples were lyophilized for 48 hours to remove all water and weighed (W_d). Samples were then immersed in 10 ml of 1,4-dioxane for 24 hours and freeze dried and weighed (W_s). Sol fraction of the hydrogel composites was determined by using following equation :

$$\text{Sol fraction} = \frac{W_d - W_s}{W_d} * 100 \quad (2.1)$$

Sol gel fraction is a measure of the unreacted monomers after crosslinking.

2.4.2 Swelling Ratio

The samples were prepared as previously described in the sol study. Briefly, CPEGMC/HA with different concentration were fabricated. The films were cut into circular discs of diameter 10 mm and 2mm thickness ($n = 8$). The samples were freeze dried for 2 days to ensure the removal of all water. The samples were weighed and

recorded as W_i . Samples were then immersed in 10 ml of DI-water and at predefined time points removed from the DI-water and weighed again (W_d). The samples were weighed until the equilibrium state was reached :

$$\text{Swelling ratio} = \frac{W_i - W_d}{W_i} * 100 \quad (2.2)$$

2.4.3 Degradation Profile

CPEGMC/HA films were cut into discs of dimension 10 mm x 2 mm (n = 8). The samples were dried using a freeze dryer and weighed. This was recorded as the initial dry weight (W_i). The samples were immersed in test tubes with 10 ml of PBS (pH \sim 7.4) and incubated at 37 °C and taken out at different time points. The samples were triple washed in DI-water to remove any residual salts and freeze dried. The weights were recorded again as the final weight (W_f) . The mass loss was measured as :

$$\text{Mass loss} = \frac{W_i - W_f}{W_i} * 100 \quad (2.3)$$

2.4.4 Mechanical Properties

The mechanical properties of CPEGMC/HA networks were studied under compression using the MTS Insight II mechanical tester fitted with a 10 N load cell. The specimens were prepared by placing the crosslinking mixture into cylindrical vials of 12 mm outer diameter and 10 mm inner diameter. The cylindrical non-hydrated samples (10 mm x 10 mm, width x thickness) were compressed at a rate of 1 mm/min to 50% of the original thickness. Hydrated CPEGMC/HA samples were also subjected to compressive mechanical testing. The crosslinked CPEGMC/HA samples were soaked in water till equilibrium mass and then compressed at a rate of 1 mm/min to 50% of the original thickness. Hydrated CPEGMC/HA samples were also subjected to 10 cycles of compressive testing where the samples were compressed to 20% of the original thickness. Values were converted to stress- strain and the initial modulus was calculated from the initial gradient of the curve (0-10% compression). The results are presented as mean standard \pm standard deviation (n = 5).

2.5 CPEGMC/HA Scaffold Pore Morphology

To characterize the presence of pores in the composite surface, the CPEGMC/HA films were soaked in DI water overnight. The samples were then placed in cryo molds and embedded in OCT. The samples were then cryosectioned and the pictures were taken under a microscope to characterize the pore morphology.

2.6 In Vitro Mineralization

The CPEGMC and CPEGMC/HA samples were incubated in 10ml of 5x Simulated Body Fluid (SBF) prepared as previously mentioned [34, 35, 36]. The samples were taken out at day 1 and day 7. The samples were triple rinsed with DI water to remove excess salt. The samples were air dried, sputter coated and analyzed under a scanning electron microscope (HITACHI 3000N SEM). The elemental composition of the surface CPEGMC and CPEGMC/HA films were verified by using EDX.

Table 2.1. Chemical composition of 1x SBF as mentioned in Tas et.al

Order	Reagent	Amount(gpl)
1	NaCl	6.547
2	NaHCO ₃	2.268
3	KCl	0.373
4	Na ₂ HPO ₄ .2H ₂ O	0.178
5	MgCl ₂ .6H ₂ O	0.305
6	CaCl ₂ .2H ₂ O	0.368
7	Na ₂ SO ₄	0.071
8	(CH ₂ OH) ₃ CNH ₂	6.057

2.7 Osteoblast Culture

Human fetal osteoblasts (hFOB 1.19) were purchased from American Type Culture Collection (ATCC). The cells were cultured according to ATCC protocol. hFOB 1.19 cells were cultured in phenol free Dulbecco's modified Eagle's medium (DMEM)-Ham's F12 1:1 medium supplemented with 10% fetal bovine serum (FBS)(HyClone) and geneticin (300 μ g/ml; Sigma-Aldrich, St.Louise) at 37°C.

2.8 Osteoblast Surface Seeding on CPEGMC/HA

CPEGMC/HA films were modified by covalently crosslinking collagen on the surface. The -COOH group of the PEGMC film was activated by immersing the films in 5 mg/ml EDC solution for 1 hour at 4 °C. The films were then coated with 0.5 mg/ml collagen PBS solution for an additional 4 hours. The samples were then freeze dried. The samples were then sterilized by soaking the samples in 70% ethanol for 30 minutes followed by three successive washes with PBS. The films were placed under UV light for 1 hour after which they were soaked in osteoblast media overnight. hFOB was trypsinized and seeded at a density of 200,000 cells/ml. Cell culture was maintained under standard culture conditions (37 °C, 95% relative humidity, and 5% humidity) for 2 days. The samples were taken out on day 1 and day 2. The films were fixed with 3% glutaraldehyde and dehydrated using increasing concentrations of ethanol (50%, 70%, 90%, 95% and 100%) followed by lyophilization. The samples were analyzed under the SEM to determine cellular attachment and morphology.

2.9 Osteoblast Encapsulation

CPEGMC/HA crosslinking solution was prepared by adding PEGMC, HA and PEG-DA 3400 to make a uniform solution. Osteoblasts (hFOB 1.19) were trypsinized and resuspended in cell culture media to make a final concentration of 12 million/ml. Cell suspension was added to the polymer solution followed by the addition of the APS/TEMED redox initiators (25 mM concentration). The cell-polymer solution was incubated at 37 °C for 15 minutes until gelation. Two cellular groups were prepared, CPEGMC hydrogel and CPEGMC/HA hydrogel. The samples were then cut into small circular discs of equal dimension and placed in a 6 well plate and covered in

media. The hydrogel cell constructs were placed in sub culture and taken out at day 7, 14 and 21 and stained using LIVE/DEAD assay (Molecular Probes). Cell viability and distribution were observed under a fluorescent microscope [37].

2.9.1 DNA Assay

The PicoGreen assay (Molecular Probes) was used to measure the double stranded DNA content of the CPEGMC hydrogels encapsulated with hFOB 1.19 osteoblasts. At various time points, the hydrogel constructs were removed from media and homogenized in PBS by using forceps. 500 μ l of 0.2% Triton-X100 solution was added to the hydrogel constructs. The samples were subjected to two freeze-thaw cycles. The homogenates were then sonicated for 30 sec to evenly distribute DNA throughout the solution. The homogenates were centrifuged for 10 minutes at 4000 rpm. The supernatant after centrifuging was used to measure the DNA content of each cell/polymer construct using PicoGreen assay according to the protocol instructions. Results are presented as μ g DNA and samples were performed in triplicate [38, 37].

2.9.2 ALP Activity Assay

The hydrogel constructs were washed with PBS. The constructs were then homogenized using forceps. Alkaline buffer solution was added to the constructs and sonicated to ensure that the constructs were completely homogenized. The lysate was centrifuged at 4000 rpm for 10 min at 4 °C. 100 μ l of supernatant was incubated with 100 l of p-nitrophenyl phosphate solution in a 96 well plate at 37°C for 1 hour. The reaction was stopped by adding 0.2M NaOH solution to each well. The production of p-nitrophenyl in the presence of ALP was measured by monitoring the light

absorbance at 405 nm by using microplate reader (Infinite 200, Tecon Group Ltd, Switzerland) [39].

2.9.3 Analysis of Calcium Content

The hydrogel constructs were washed with PBS and homogenized. The supernatant was collected and 50 μ l of the supernatant was added to a 96 well plate. The calcium concentration of the cell lysate was analyzed using cresolphthalein complexone (Sigma). After 10 minutes of addition of reagents the absorbance was read at 575 nm using a microplate reader (Infinite 200, Tecon Group Ltd, Switzerland) [39].

2.10 Drug Release Study

Desferrioxamine (DFO) drug release was studied by encapsulating the highly water soluble drug in the PEGMC polymer gel. DFO has been shown to increase angiogenesis and promote bone regeneration when injected in vivo in distraction gap by activation of the hypoxia-inducible factor-1 α (HIF-1 α) pathway. HIF-1 α pathway was found to play an important role in promoting angiogenesis and osteogenesis in bone healing [40]. The drug concentration was 100 mg/ml. The polymer was crosslinked in a 96 well plate with each well having 200 μ l of polymer-drug solution. The CPEGMC films were incubated in 2 ml of PBS and placed on a orbital shaker (VWR Incubating Shaker, 60 rpm) where the temperature was maintained at 37 °C. 1 ml of PBS was taken out at different time points and the volume was replaced to 2 ml. The drug concentration was quantified by adding excess FeCl₃ to the PBS solution and read using a spectrophotometer (Infinite 200, Tecon Group Ltd, Switzerland) at

a wavelength of 420 nm [41].

2.11 Statistical Analysis

Data was expressed as mean \pm standard deviation. The statistical significance between two sets of data was calculated using one way ANOVA. Data were taken to be significant, when $p < 0.05$ was obtained.

CHAPTER 3

RESULTS

3.1 Polymer Characterization

PEGMC was synthesized by a simple polycondensation reaction between the monomers citric acid, maleic anhydride and PEG ($M_w=200$ Da). Different molar ratios of PEGMC prepared in this study are shown in Table 1. PEGMCs synthesized based on different stoichiometric ratios of citric acid to maleic anhydride all resulted in transparent viscous liquid at room temperature after the initial polycondensation reaction. All the different PEGMCs were found to be water soluble. The synthesis time increased from 4 to 10 hours with increasing maleic anhydride monomer content. To confirm the presence of various functional groups in the prepolymer, FT-IR analysis was done on PEGMCs. The presence of the vinyl peak at 1640 cm^{-1} proved the successful incorporation of the vinyl group from the maleic anhydride. In addition, the presence of the hydrogen bonded -OH at 3570 cm^{-1} and C=O of the carboxyl group at $1690\text{-}1750\text{ cm}^{-1}$ confirmed there are available -OH/-COOH for further bio-functionalization.

The chemical structure of the PEGMC was characterized by analyzing the resonance of the various hydrogen atoms in the PEGMC backbone and their resultant chemical shifts of the $^1\text{H-NMR}$ peaks with tetramethylsilane (TMS) as the reference. The peaks labeled at a) located between 6 - 7 ppm were assigned to the $-\underline{\text{C}}\text{H} = \underline{\text{C}}\text{H}-$ of the maleic anhydride. The peaks (b) at 3.1 - 2.65 ppm were assigned to the $-\underline{\text{C}}\text{H}_2$ of the citric acid. The peaks (d) located at 4 - 4.5 ppm was assigned to $-\text{O}-\text{CH}_2\underline{\text{C}}\text{H}_2$ of the poly(ethylene glycol). The chemical compositions of the prepolymers were de-

terminated by integrating the area under the peaks of the characteristic proton from each monomer : maleic anhydride ($a/2$), citric acid ($b/4$), and diol ($d/4$). The incorporation of higher maleic anhydride showed increasing peak intensity suggesting that the PEGMC prepolymer has terminal vinyl groups. As shown in Table 1, the feed ratio and the actual polymer composition shows that the vinyl group is not completely incorporated into the polymer chain. Thus the composition of the prepolymer can be controlled to a large degree by changing the feeding ratios of the monomers participating in the reaction.

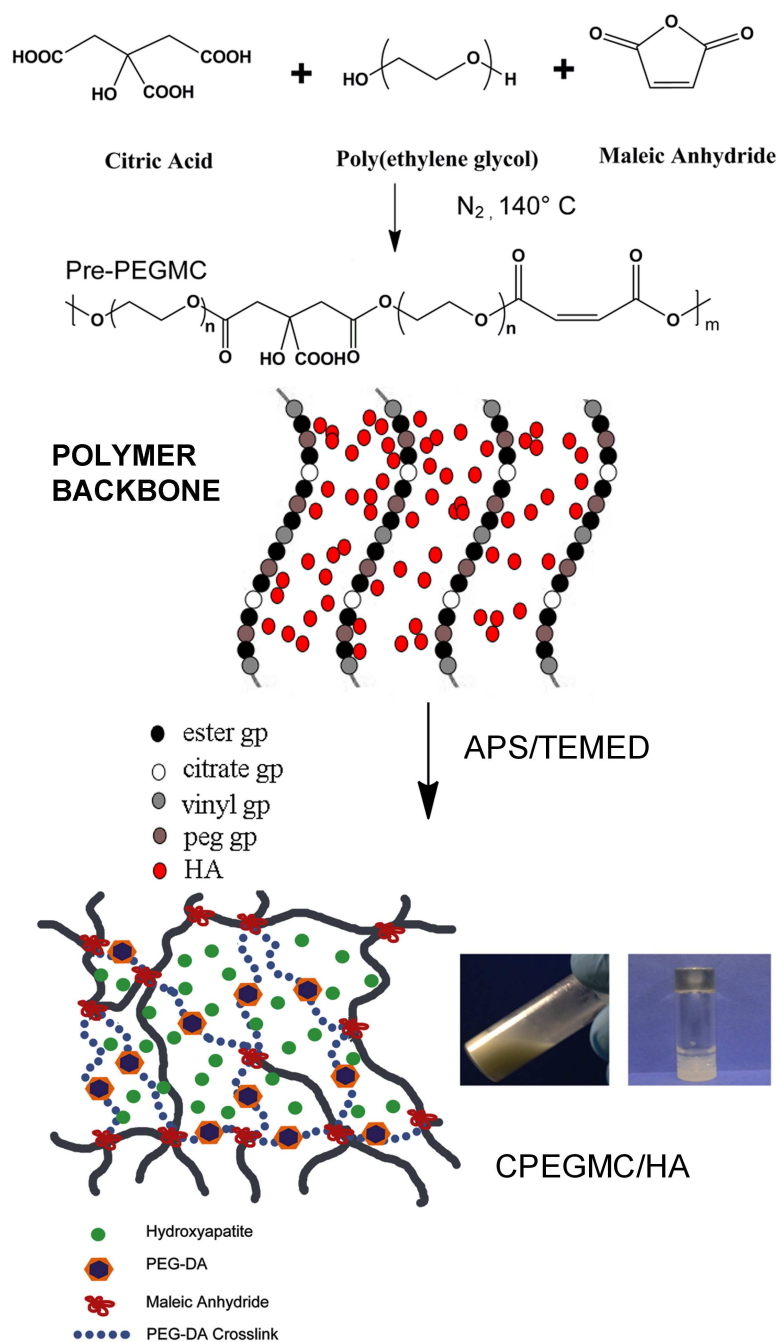


Figure 3.1. Synthesis schematic of PEGMC. PEGMC prepolymer was synthesized by a simple polycondensation reaction using the monomers citric acid, PEG and maleic anhydride. Redox polymerization using APS/TEMED was used to fabricate the CPEGMC films. HA was added to the crosslinking solution to make CPEGMC/HA films.

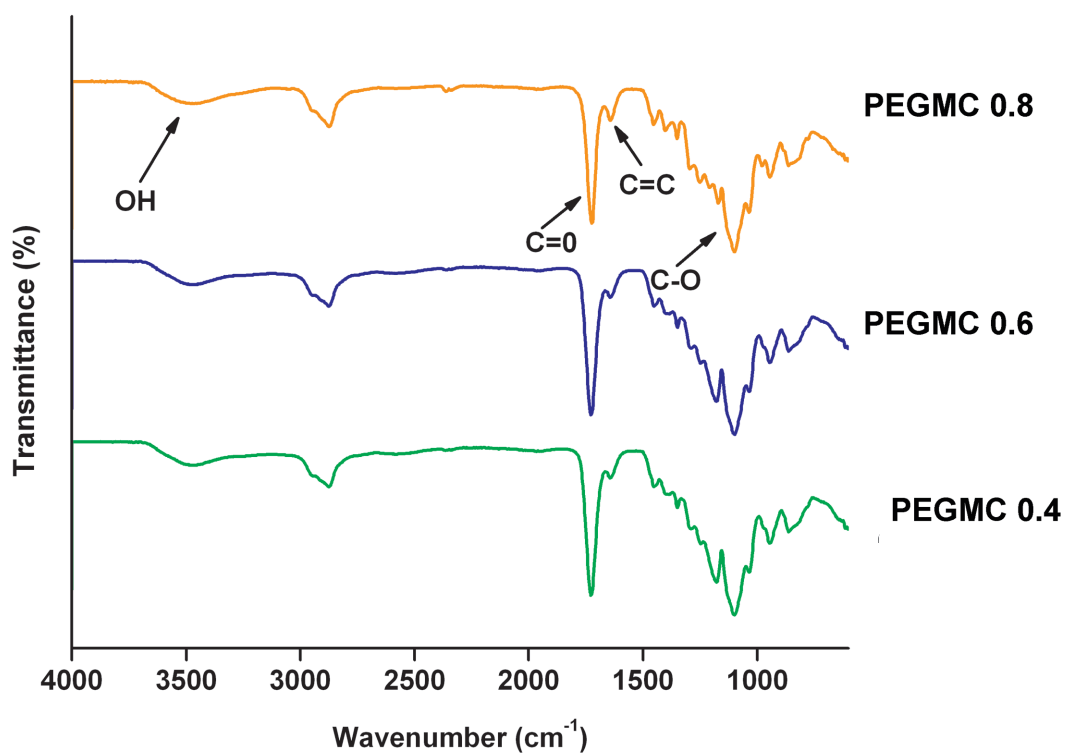


Figure 3.2. FT-IR spectra of PEGMC prepolymers.

Table 3.1. Feed ratios and actual molar composition of different PEGMCs where MA and CA denote Maleic Anhydride and Citric Acid respectively.

Polymer	Feed Ratio (mol)			Composition (mol)		
	MA	CA	PEG	MA	CA	PEG
PEGMC 0.4	0.2	0.3	0.5	0.12	0.35	0.5
PEGMC 0.6	0.3	0.2	0.5	0.27	0.26	0.5
PEGMC 0.8	0.4	0.1	0.5	0.32	0.13	0.5

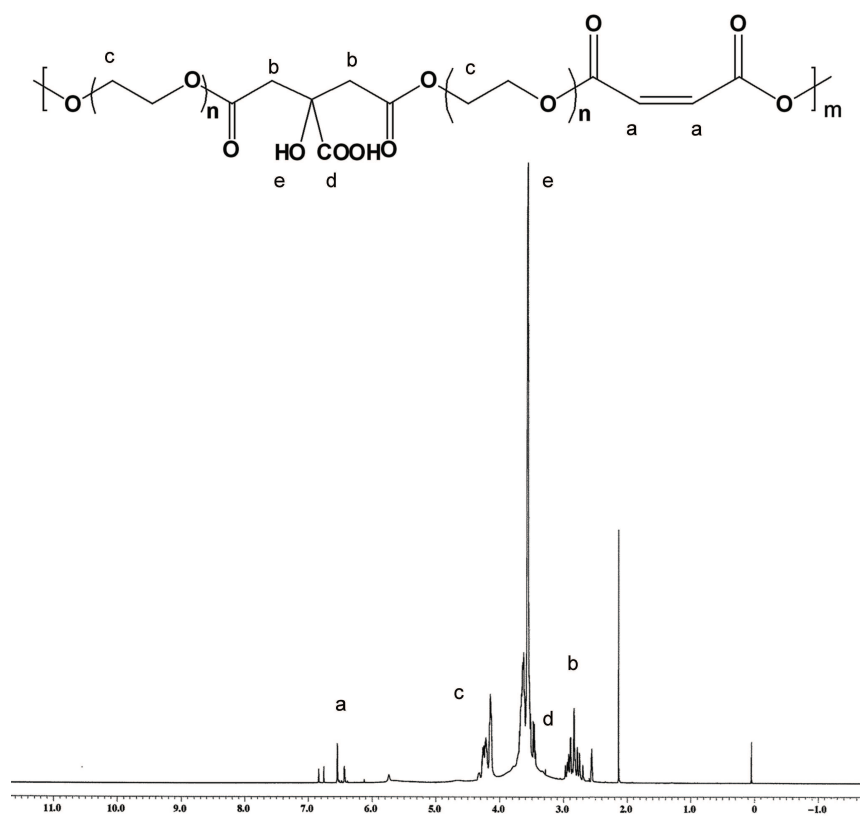


Figure 3.3. ¹H-NMR spectra of PEGMC 0.6.

3.2 Preparation and Characterization of CPEGMC/HA

Redox crosslinked CPEGMC/HA networks were polymerized by free radical polymerization. The presence of a reduced peak at 1640 cm^{-1} compared to PEGMC in the FT-IR spectra was due to the vinyl group of the maleic anhydride. The FT-IR spectra also confirmed that the pendant hydroxyl and carboxyl groups of the citric acid were preserved.

3.2.1 Sol Content

Sol content of CPEGMC/HA network is shown in Fig 3.4. There was no significant difference in the sol content with increase in HA concentration. The sol content for CPEGMC/HA(30) was $6.90 \pm 0.74\%$. The sol content for CPEGMC/HA(60) was $5.66 \pm 1.13\%$. This suggests that HA does not contribute to the sol content and does not leach out from the polymer network.

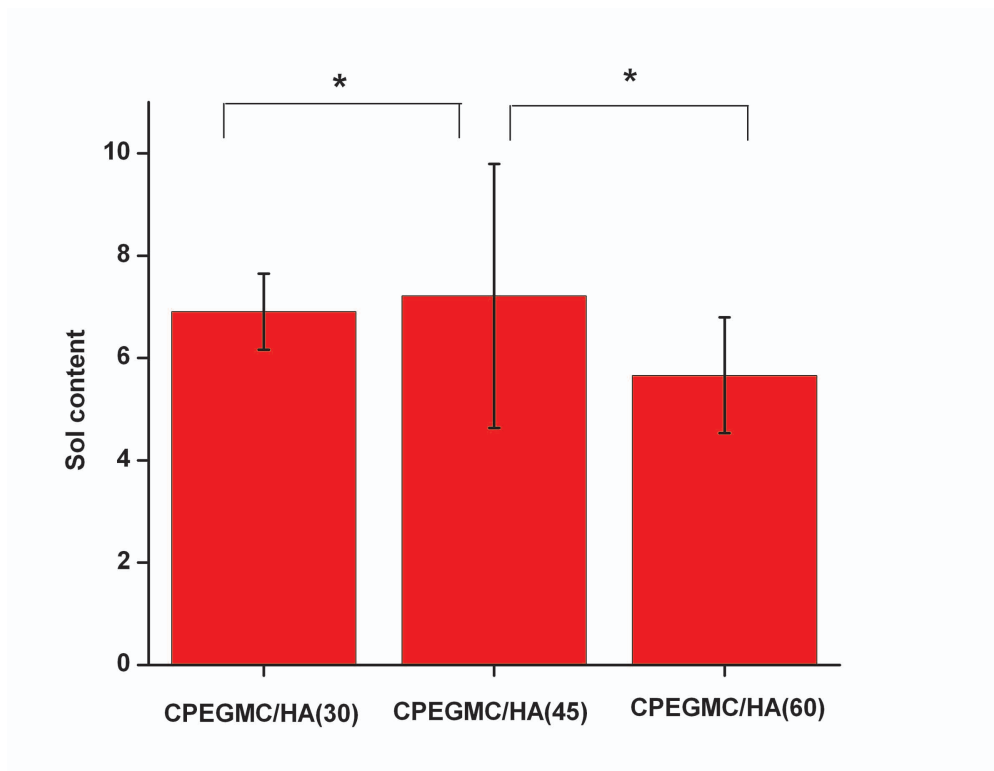


Figure 3.4. Sol content of CPEGMC/HA where PEGMC 0.6 was crosslinked with different HA concentration. Error bars represent standard deviations ($n = 8$). * corresponds to $p < 0.05$.

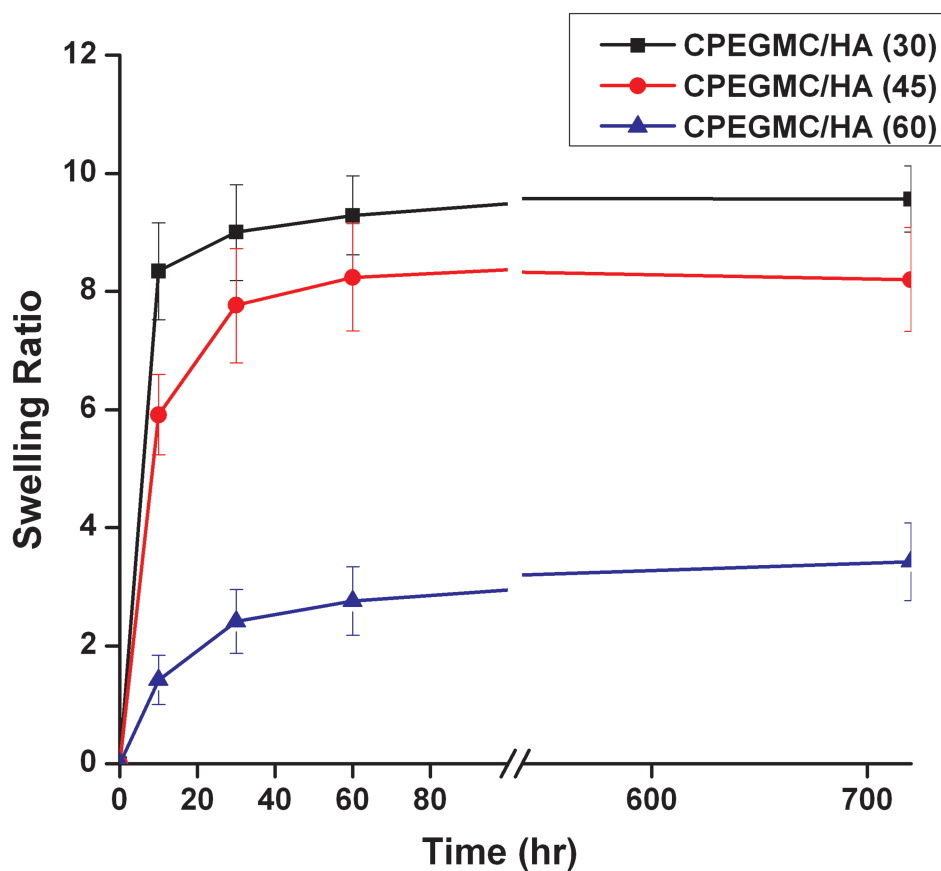


Figure 3.5. Swelling ratio of CPEGMC/HA where PEGMC 0.6 was crosslinked with different HA concentrations. Error bars represent standard deviations ($n = 8$).

3.2.2 Swelling Ratio

Swelling study for different compositions of CPEGMC/HA indicates that the swelling ratio reduces with increasing HA concentration. As the HA is uniformly dispersed in the polymer network, the space between crosslinks for water uptake is diminished. Thus the swelling ratio reduces from 9.56 ± 0.56 to 3.42 ± 0.66 for CPEGMC/HA(30) and CPEGMC/HA(60).

3.2.3 Degradation Profile

Degradation profile for CPEGMC/HA network showed increasing mass loss with lower concentration of HA. CPEGMC/HA (30) showed a mass loss of $58.18 \pm 6.60\%$ at the end of 22 weeks. The higher concentration composite CPEGMC/HA(60) resulted in a mass loss of $32.24 \pm 1.79\%$ at the end of 22 weeks. This indicates that the polymer network loses mass primarily due to the degradation of the polymer and that HA does not leach out from the network in significant amounts. This was evident as there was no visible presence of HA in the PBS solution used to incubate the samples for the degradation study. Repeated centrifugation to collect and quantify the extent of HA leaching out of the system in the course of degradation did not result in any quantifiable amount. The degradation of the polymer network preserved the form and shape of the construct through the entire 22 weeks of duration of the study.

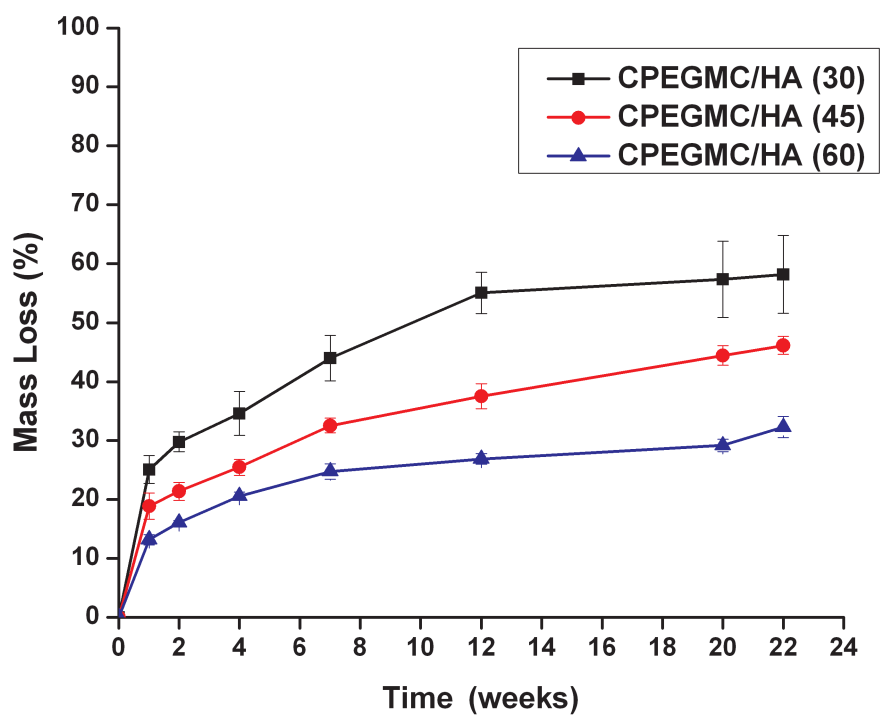


Figure 3.6. In vitro degradation of CPEGMC/HA where PEGMC 0.6 was crosslinked with different HA concentrations in PBS (pH 7.4; 37 °C). CPEGMC/HA was crosslinked using APS/TEMED redox initiators using PEG-DA 3400 as a crosslinker.

3.2.4 Mechanical Properties

Mechanical compressive tests of CPEGMC/HA showed that the polymer network was elastic and achieved complete recovery without any deformation for hydrated and non-hydrated conditions. Compressive mechanical properties for non hydrated and hydrated CPEGMC/HA constructs showed complete recovery when the compressive load was removed. The peak compressive modulus for CPEGMC/HA (30) when hydrated was 0.012 ± 0.005 MPa. The modulus for non-hydrated CPEGMC/HA(30) (0.01 ± 0.005 MPa) was similar to the modulus when hydrated. There was no difference between the hydrated and non-hydrated modulus for CPEGMC/HA(45) (0.026 ± 0.12 MPa). However there was an increase in the modulus of the hydrated (0.10 ± 0.02 MPa) and non-hydrated (0.20 ± 0.03 MPa) CPEGMC/HA(60) samples. Thus the mechanical strength of the composites does not decrease significantly when hydrated. Fully hydrated CPEGMC/HA samples when subjected to ten continuous cycles of compression were found to withstand the test without breaking and also recovered its original state. Thus the PEGMC confers the constructs with the elastic property and the HA provides the increased strength.

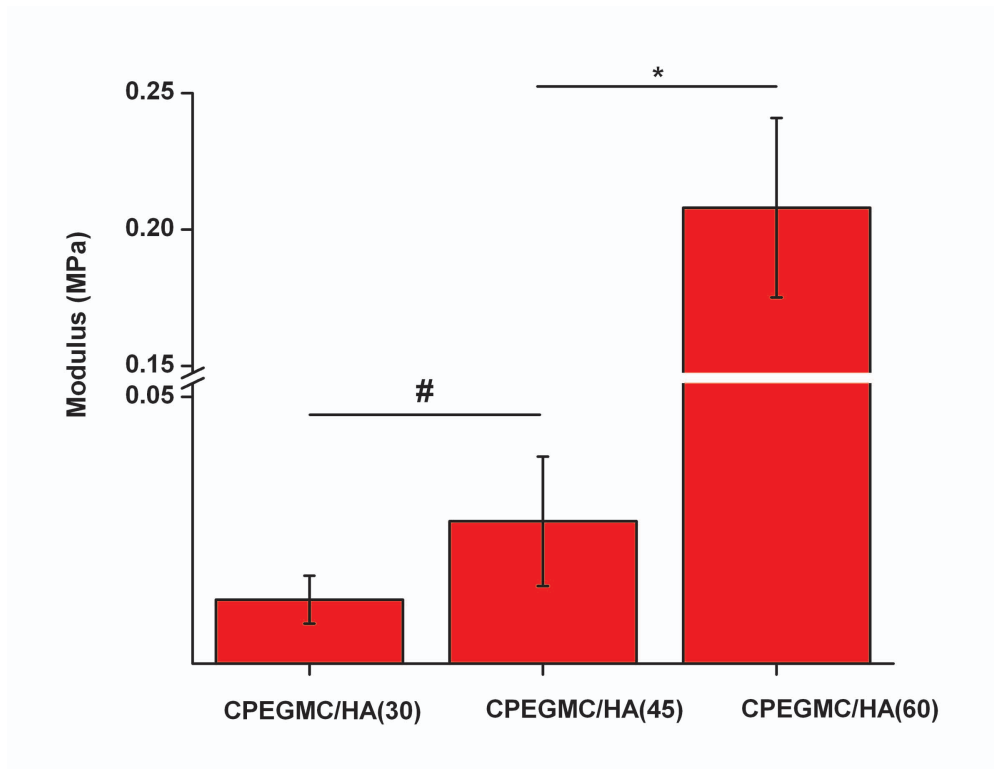


Figure 3.7. Compressive modulus of non hydrated CPEGMC/HA where PEGMC 0.6 was crosslinked with different HA concentrations. * corresponds to $p < 0.05$ and # represents $p < 0.01$.

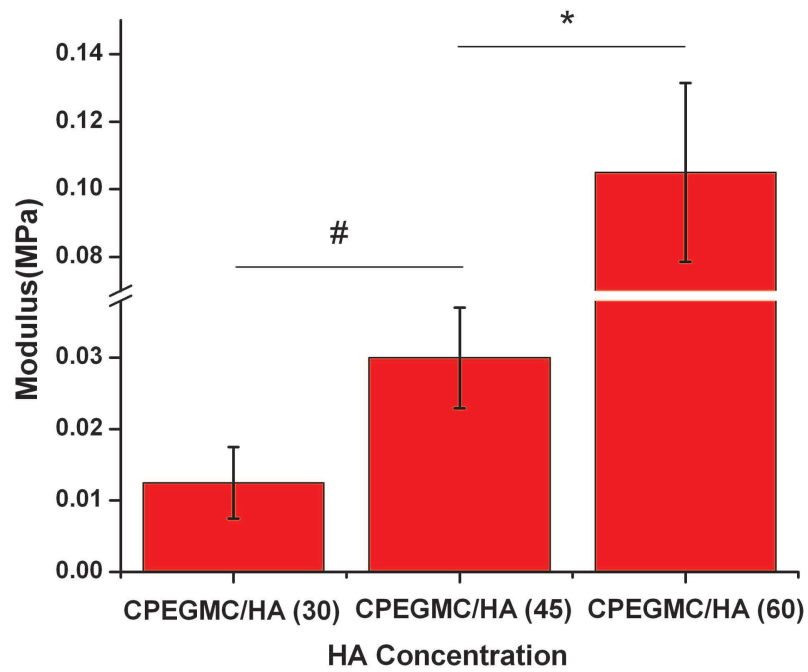


Figure 3.8. Compressive mechanical strength of CPEGMC/HA when fully hydrated where PEGMC 0.6 is crosslinked with different HA concentrations. The CPEGMC/HA composites were immersed in DI-water till weight equilibrium was reached and then tested. * corresponds to $p < 0.05$ and # represents $p < 0.01$.

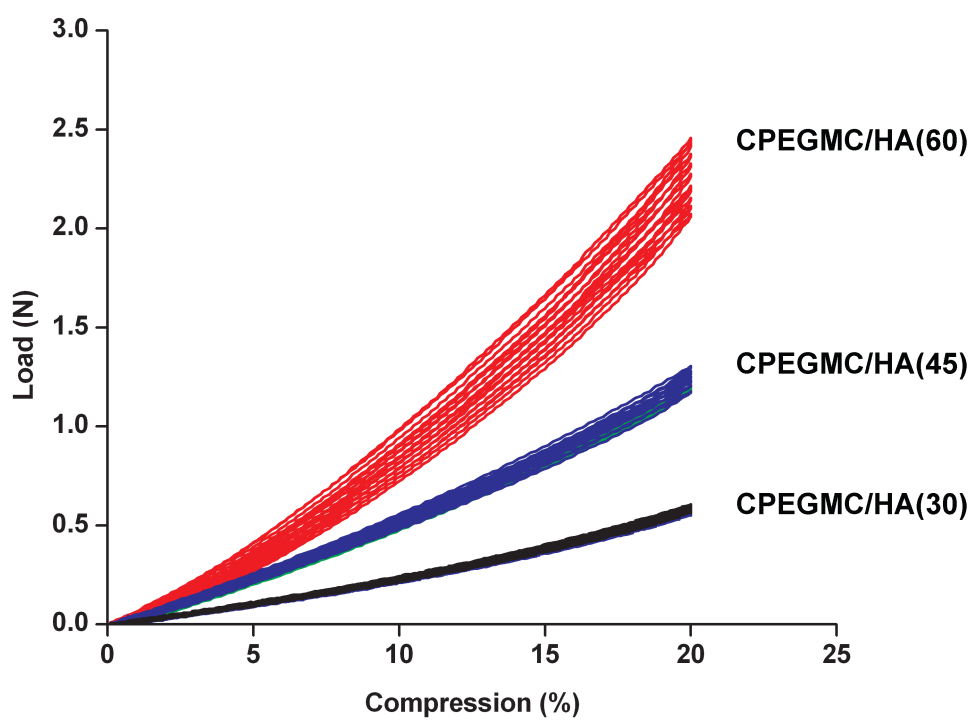


Figure 3.9. Hysteresis of CPEGMC/HA films where PEGMC 0.6 was crosslinked with different HA concentrations. The samples were loaded to 20% strain and the load was held for 30 seconds before the samples were unloaded.

3.3 CPEGMC/HA Scaffold Pore Morphology

The porous network of the CPEGMC and CPEGMC/HA were studied after the samples were completely hydrated by soaking overnight in water. The samples were frozen in OCT and cryosectioned and observed under the microscope. The CPEGMC film in Fig 3.10(A) showed a highly porous network. The CPEGMC/HA films in fig 3.10 (B), (C) and (D) are CPEGMC/HA (30), CPEGMC/HA(45) and CPEGMC/HA(60) respectively. The black shapes represent HA and are found to be uniformly distributed throughout the polymer network. The polymer outline can be clearly seen in the figures. Microphotographs shows the polymer network in the presence of HA to be highly porous with large and small pores.

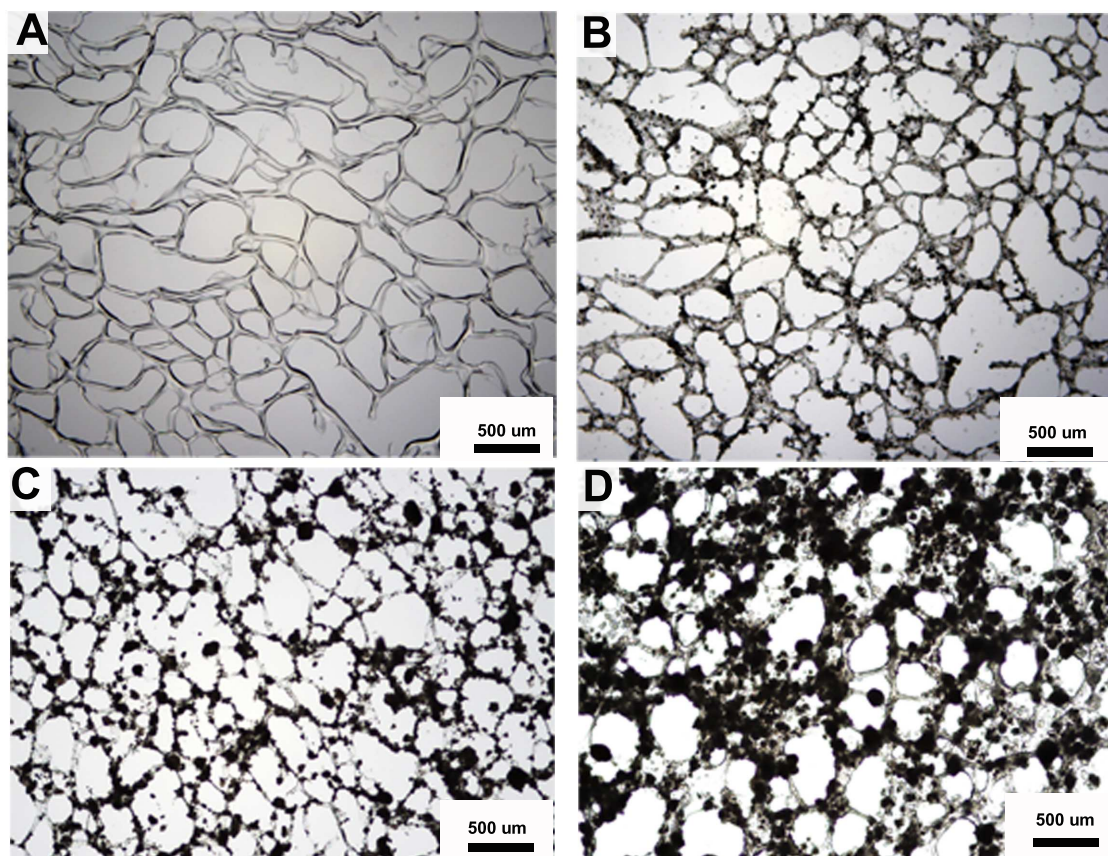


Figure 3.10. Characterization of pore morphology in CPEGMC scaffolds with different HA concentrations. Fig A), B), C) and D) shows microphotographs of CPEGMC 0.6, CPEGMC/HA (30), CPEGMC/HA (45) and CPEGMC/HA (60) when hydrated and cryosectioned to show the porous morphology.

3.4 In Vitro Mineralization

The CPEGMC and CPEGMC/HA(45) films were incubated in 5x at 37 °C. simulated body fluid(5X SBF) for a duration of 7 days. The SEM/EDS analysis of the constructs shows that there is no significant presence of CaP minerals on the surface of the CPEGMC films. However the CPEGMC/HA(45) films were covered with small dome shaped structures at the end of Day 1 as shown in Fig 3.11 (c). The Day 7 (Fig 3.11 (D)) CPEGMC/HA construct showed that surface to be completely covered in bigger but similar domed shaped structures as seen on Day 1. To confirm that the structures on the film were indeed CaP minerals, elemental analysis of the surface was done. The elemental analysis of the CPEGMC films with that of CPEGMC/HA(45) films before and after soaking in 5X SBF shows a marked increase in the wt% of Ca and P.

Table 3.2. Elemental analysis of CPEGMC and CPEGMC/HA films before and after incubation in 5X SBF at day 7

	No SBF			5X SBF (Day 7)		
	C(Wt%)	Ca(Wt%)	P(Wt%)	C(Wt%)	Ca(Wt%)	P(Wt%)
CPEGMC	27.52	0.63	0.94	76.17	12.96	1.67
CPEGMC/HA	29.33	13.3	0.97	6.73	61.13	3.61

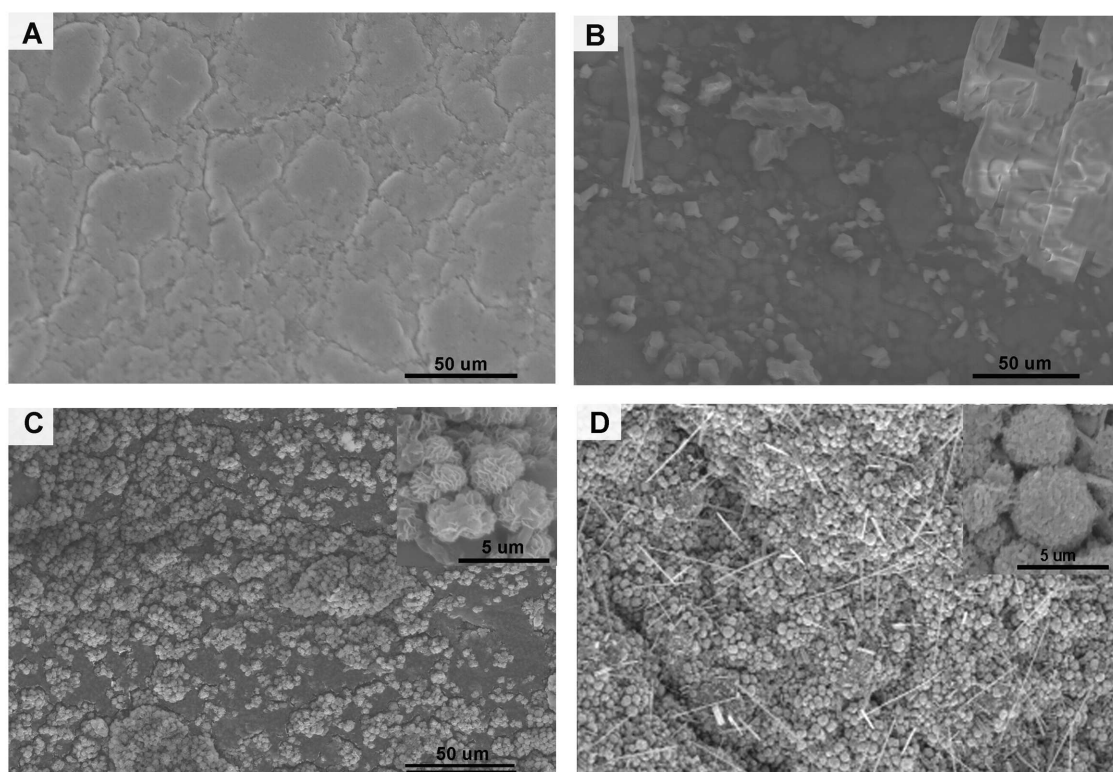


Figure 3.11. In vitro mineralization of CPEGMC/HA films when incubated in 5X SBF for 7 days. Fig A) and B) shows SEM image of the surface of CPEGMC 0.6 films when incubated in 5x SBF at day 1 and day 7 respectively. Fig C) and D) shows SEM image of the surface of CPEGMC/HA (45) when incubated in 5x SBF at day 1 and day 7 respectively. Fig C) and D) shows the entire surface of CPEGMC/HA covered with CaP minerals.

3.5 Cellular Studies

3.5.1 Osteoblast Surface Seeding on CPEGMC/HA

PEG based hydrogels do not support cell adhesion due to low protein adsorption [38]. To enhance cellular adhesion CPEGMC and CPEGMC/HA(45) films were modified by covalently immobilizing collagen on the surface. FT-IR spectrum confirms the covalent crosslinking of collagen on the polymer surface (Fig 3.12). Cellular morphology of osteoblasts seeded on CPEGMC and CPEGMC/HA (45) films were found to be mostly rounded after 4-8 hours from the initial seeding. Remaining cell culture media was added to the cell seeded constructs after 8 hours to ensure maximum possibility of attachment. It was found that the cells on the unmodified CPEGMC and CPEGMC/HA(45) films either washed away on the addition of media or still maintained a rounded morphology at the end of day 1 of subculture. However, collagen modified CPEGMC and CPEGMC/HA(45) film showed enhanced osteoblast surface attachment. Figure 3.13 , shows photomicroscopes of hFOB 1.19 osteoblasts on collagen modified CPEGMC/HA(45) stained with CFDA-SE tracer dye films after day 2 of subculture. CFDA-SE dye stains live cells green as seen in Figure 3.13(A) and (B). The SEM pictures confirm the presence of the osteoblast attachment and spreading on the collagen modified surface (Figure 3.13 (C) and (D)).

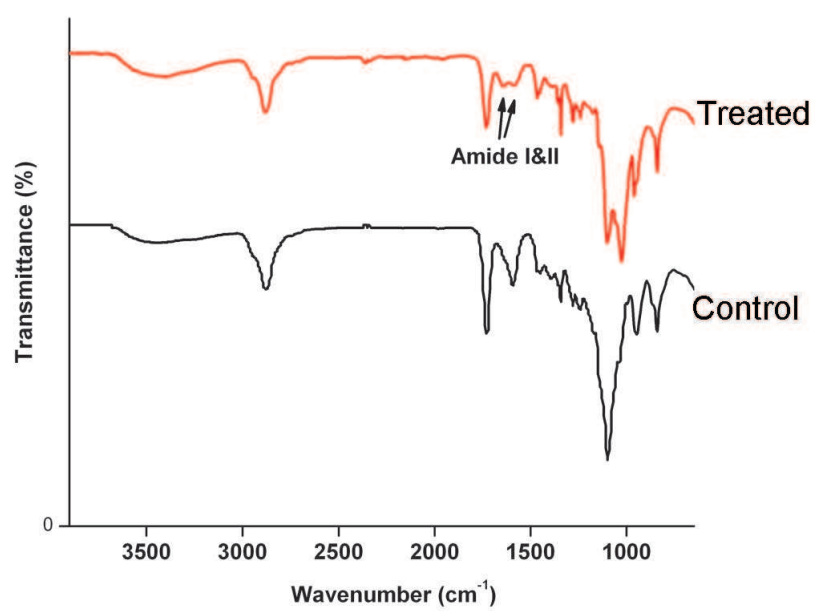


Figure 3.12. FTIR spectra of CPEGMC 0.6 and collagen modified CPEGMC films.

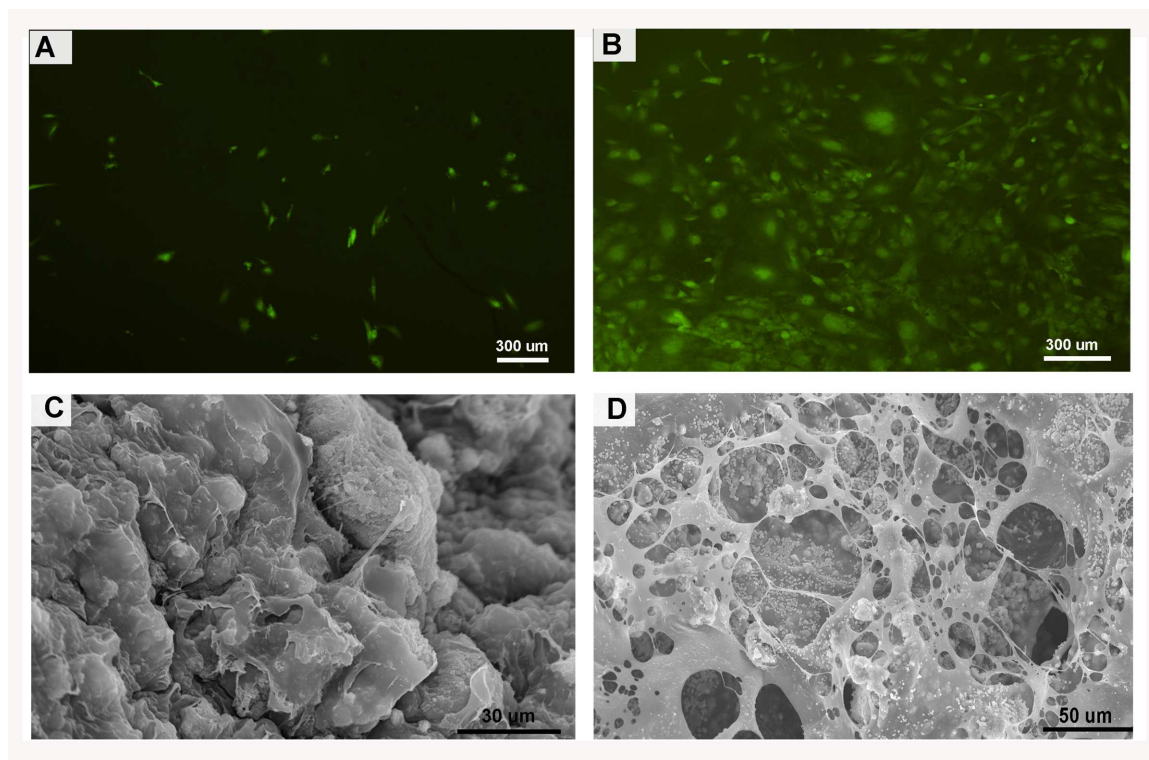


Figure 3.13. Fig A) CFDA-SE dye stained hFOB 1.19 seeded on CPEGMC/HA film after day 2 of subculture. Fig B) CFDA-SE dye stained collagen modified CPEGMC/HA surface seeded with hFOB 1.19 after day 2. Fig C) and D) SEM images of hFOB 1.19 surface seeded on CPEGMC/HA surface and collagen modified CPEGMC/HA surface respectively.

3.5.2 Osteoblast Encapsulation

Human fetal osteoblast hFOB 1.19 (ATCC) were encapsulated in CPEGMC and CPEGMC/HA (30) films. Osteoblasts hFOB 1.19 were mixed in crosslinking mixture with redox initiators (APS/TEMED) and polymerized. The networks were found to crosslink in < 15 minutes when incubated at $37\text{ }^{\circ}\text{C}$. Fluorescent photomicrographs of the encapsulated osteoblasts were taken after staining the hydrogel networks with LIVE/DEAD assay (Molecular Probes, Invitrogen) where live cells fluoresce green and cells that are not viable fluoresce red. As shown in Figure 3.14(A) : Osteoblasts encapsulated after day 1 in CPEGMC/HA were cryosectioned and stained with hemotoxylin and eosin. The figure shows uniform distribution of cells within the polymer/HA network. Figure 3.14(B) shows the SEM picture osteoblasts cell attached and spread within the cryosectioned CPEGMC/HA film. Figure 3.14(C) and (D) show CPEGMC/HA and Figure 3.14 (D) and (F) show CPEGMC with osteoblasts encapsulated on day 7 and day 21. Figure 3.14 (C),(D),(E) and (F) showed that the majority of the osteoblasts fluoresce green indicating promising cellular viability of the polymer PEGMC, HA, PEG-DA 3400 and also the redox polymerization conditions. Osteoblasts encapsulated in CPEGMC/HA (30), Figure 3.14(D) shows cellular clumps and spreading of osteoblasts indicating that HA has a positive effect on the osteoblasts.

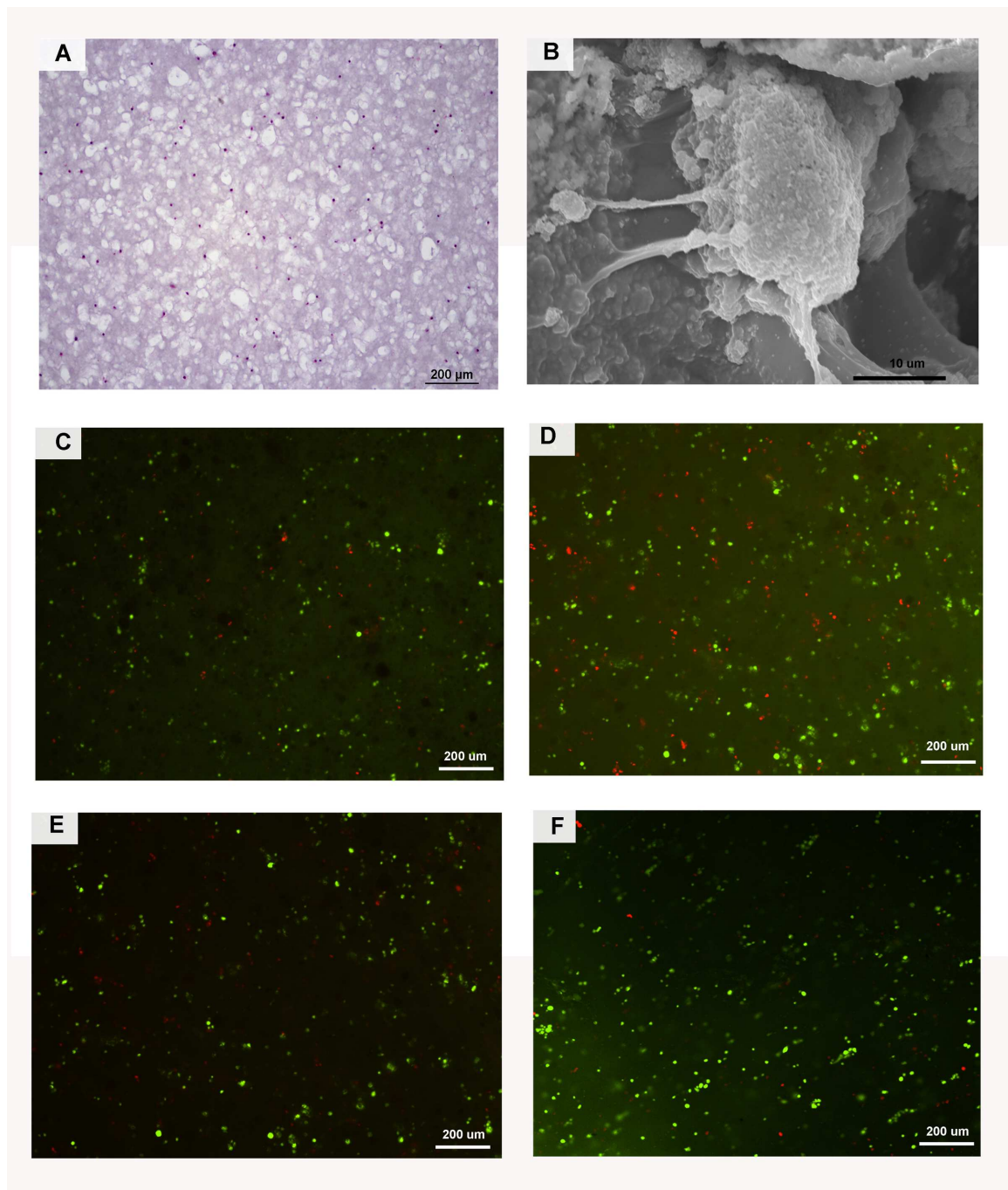


Figure 3.14. Human fetal osteoblast hFOB 1.19 were encapsulated using polymerization in CPEGMC and CPEGMC/HA hydrogels. Viability was assessed using LIVE/DEAD assay. Living cells fluoresce green whereas dead cells fluoresce red. Fig A) cryostat section of CPEGMC/HA encapsulated with cells stained with H and E shows even distribution of cells in the polymer HA matrix. Fig B) SEM image of encapsulated cell. Fig C) and D) LIVE/DEAD stained CPEGMC/HA hydrogels at day 7 and day 21. Fig E) and F) LIVE/DEAD stained CPEGMC hydrogels at day 7 and day 21.

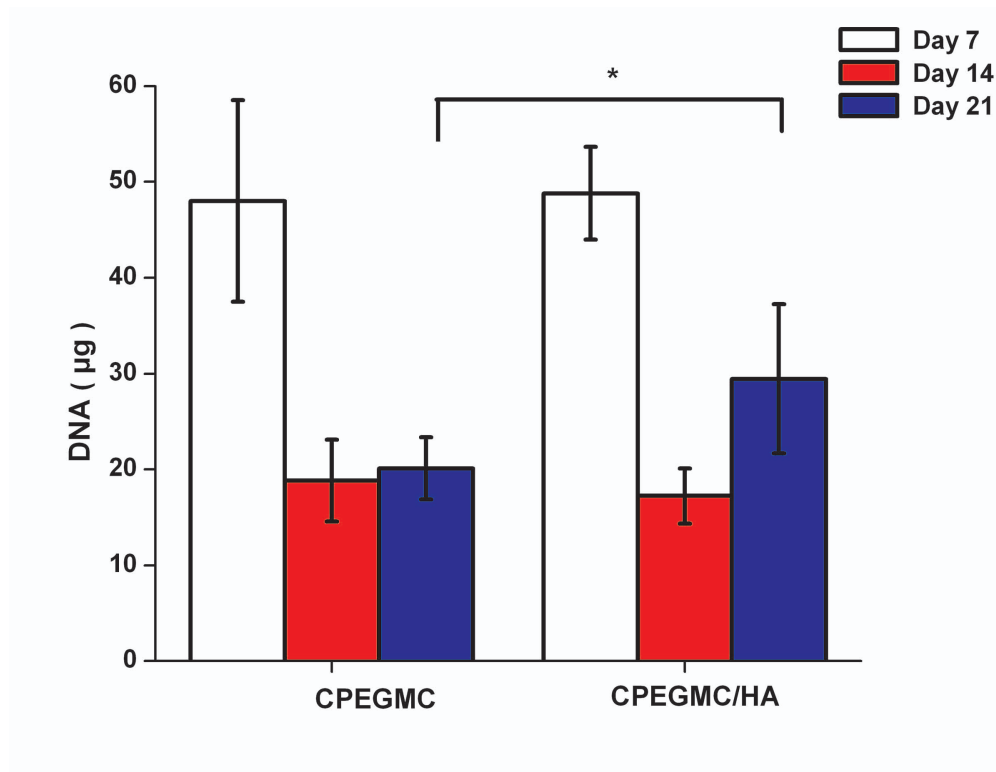


Figure 3.15. DNA content of cell/polymer (CPEGMC and CPEGMC/HA) constructs at days 7, 14 and 21. Samples were performed in triplicate. * represents $p < 0.05$.

3.5.2.1 DNA Assay

DNA content of hydrogels containing osteoblasts was assessed using PicoGreen assay and the results are as shown Fig 3.15. At the end of Day 21 of subculture the DNA content in CPEGMC/HA was greater than that seen in CPEGMC.

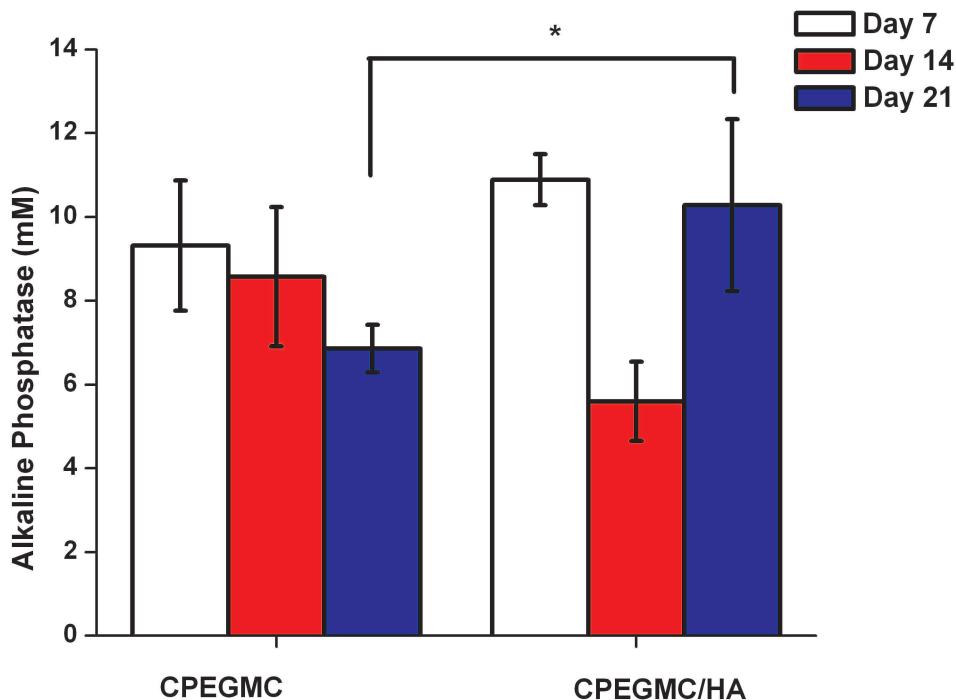


Figure 3.16. ALP content of cell/polymer (CPEGMC and CPEGMC/HA) constructs at days 7, 14 and 21. Samples were performed in triplicate. * represents $p < 0.05$.

3.5.2.2 ALP Activity Assay

ALP activity was measured in CPEGMC and CPEGMC/HA (30) hydrogels. The general trend of ALP activity over 21 days of culture are as follows a) Day 7 showed CPEGMC/HA(10.89 ± 0.60 mM) to have a higher ALP activity as compared to CPEGMC (9.32 ± 1.55 mM) (b)Day 14 showed a decrease in ALP activity in both CPEGMC (8.57 ± 1.65 mM) and CPEGMC/HA(30)(5.60 ± 0.94 mM). (c)However Day 21 showed an increase in ALP activity for CPEGMC/HA(30) from Day 14. There was a significant increase in the ALP activity at day 21 between CPEGMC (6.86 ± 0.56 mM) and CPEGMC/HA(30) (10.28 ± 2.05 mM)

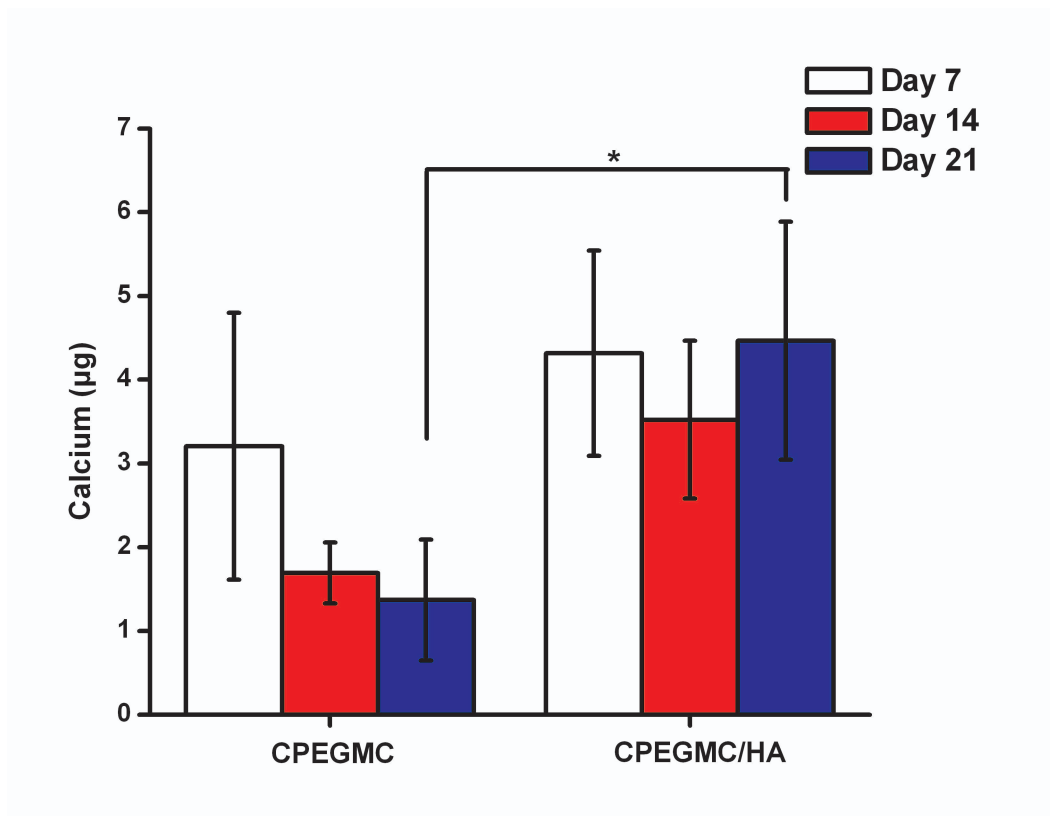


Figure 3.17. Calcium content of cell/polymer (CPEGMC and CPEGMC/HA) constructs at days 7, 14 and 21. Samples were performed in triplicate. * represents $p < 0.05$.

3.5.2.3 Analysis of Calcium Content

Calcium deposition by encapsulated osteoblasts in CPEGMC and CPEGMC/HA(30) showed a similar trend as seen for ALP activity. The general trend followed over 21 days of subculture of CPEGMC films showed a decrease in the calcium content from $3.20 \pm 1.59 \mu\text{g}$ at day 7 to $1.36 \pm 0.72 \mu\text{g}$ at day 21. The calcium content in the presence of HA decreased at day 14 to $3.52 \pm 0.94 \mu\text{g}$ from the $4.31 \pm 1.22 \mu\text{g}$ of day 7 and then again showed an increase to $4.46 \pm 1.42 \mu\text{g}$ at day 21.

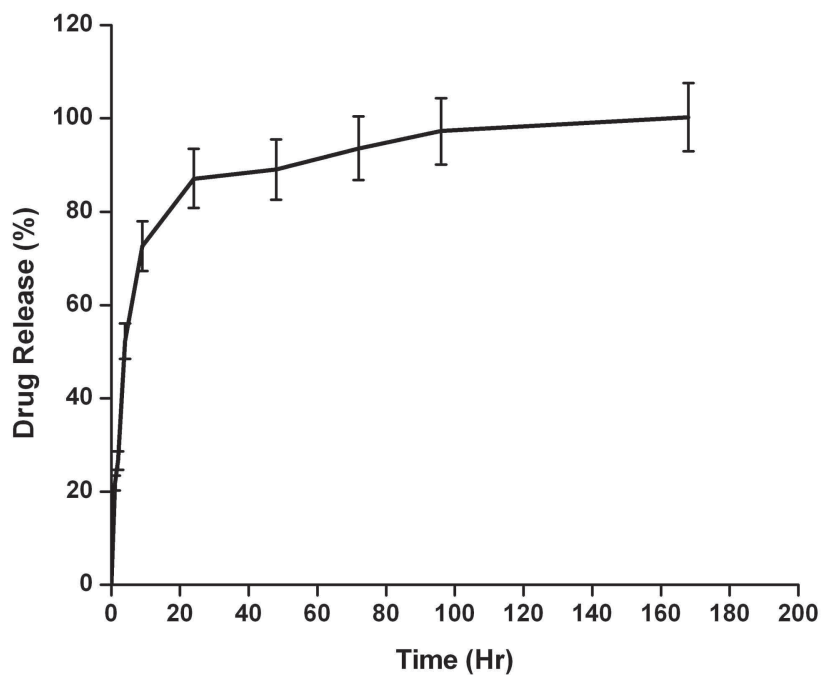


Figure 3.18. DFO drug release profile over time. Desferrioxamine was encapsulated in CPEGMC hydrogel and the release was measured over 7 days. Error bars represent standard deviation. ($n = 5$).

3.6 Drug Release Study

CPEGMC films were crosslinked with DFO drug encapsulated inside. The drug release profile from the hydrogel was studied for duration of 7 days. The photospectrometric absorbance at 440nm confirmed that 80% of the drug release occurred within the first 24 hours of incubation in PBS (pH \sim 7.4).

CHAPTER 4

DISCUSSION

In this study we have synthesized and characterized a hydrogel named PEGMC. PEGMC has many properties that make it desirable for use in bone tissue engineering applications. PEGMC is synthesized by reacting citric acid, PEG and maleic anhydride in a simple polycondensation reaction. The constituent monomers used were inexpensive, non toxic and readily available. The reaction of citric acid and maleic anhydride with PEG results in the formation of ester bonds in the prepolymer backbone which renders the prepolymer hydrolysable and hence biodegradable. The rationale behind the selection of the individual monomers include: 1) Citric acid was chosen because it is a multifunctional monomer, which when reacted with PEG can produce a polymer backbone with degradable ester bonds. The presence of pendant carboxyl and hydroxyl groups allows for future biofunctionalization. 2) Maleic anhydride was selected as a monomer to introduce vinyl group in the polymer backbone in order to crosslink the pre-polymer using free radical polymerization. 3) PEG was selected as the difunctional monomer to react with the acid to form a polyester chain. Lower molecular weight PEG was chosen as it is easier to react.

FT-IR analysis confirmed the incorporation of vinyl and ester groups in the pre-polymer and the preservation of the pendant -COOH and -OH group of the citric acid. Pre-PEGMC can be crosslinked using two different crosslinking mechanisms. The presence of the polyfunctional citric acid allows ester crosslinking of pre-PEGMC through the pendant groups. Additionally vinyl groups from maleic anhydride can be used in free radical polymerization using UV crosslinking and redox crosslinking. The

selection of the polymerization mechanism is influenced by the targeted application. Redox polymerization is more advantageous for an injectable application since the ability to direct light uniformly in different areas of the body is limited. Prolonged exposure to UV light can also damage surrounding healthy tissue which is overcome when using redox. PEGMC crosslinking was studied in detail in [1] for both redox and UV crosslinking mechanisms. It was found that CPEGMC had lower swelling properties, reduced sol content and slower degradation rates when crosslinked using redox.

In our study we designed an injectable PEGMC/HA mixture that can be crosslinked in situ using redox to yield crosslinked CPEGMC/HA. The crosslinking environment was studied in detail to ensure the fastest crosslinking time using the lowest initiator concentration. Pre-PEGMC was initially crosslinked using APS/Ascorbic acid using acrylic acid as a crosslinker. However for in situ applications it is desired that the polymer be as close to physiological pH. PEGMC is acidic with a pH \sim 1-2. The PEGMC was neutralized by adding NaHCO_3 to pH \sim 7. Under more neutral pH, APS/Ascorbic acid with acrylic acid did not result in PEGMC crosslinking. The redox initiator combination of APS/TEMED was found to be effective in crosslinking PEGMC at a neutral pH. Another important consideration was the crosslinking time. For an injectable application it is desired that the gelation time be as low as possible while keeping the initiator concentration at a minimum to ensure that the crosslinking mixture is cytocompatible. This was achieved by using polyethylene glycol diacrylate PEG-DA as a crosslinker. Mikos et.al has previously reported the cytocompatibility of different concentrations of APS/TEMED used in crosslinking oligo(poly(ethylene glycol)fumarate) (OPF). The study concluded that at higher concentrations of 100mM (APS/TEMED) and 500mM (APS/TEMED) the cell viability was less than 10% after 2 hours. Initiator concentration of 10mM was found to have

cell viability comparable to the control. To achieve rapid crosslinking (< 15 minutes) by using the least initiator concentration (25mM APS/TEMED), there was a need to introduce an additional component to the crosslinking mixture. Poly ethylene glycol diacrylate PEG-DA was chosen as the crosslinker. Different concentrations and molecular weight PEG-DA were tested. PEG-DA ($M_w=3400$ Da) was found to be most effective crosslinker. In vitro cytotoxicity tests of different molecular weight PEGDA using MSCs showed the PEG-DA 3400 showed almost 100% cells were alive at different concentrations ranging from $10\%(w/v)$ to $0.1\%(w/v)$ [31, 42, 43]. Therefore changing the polymer, crosslinker and initiator concentrations the crosslinking time can be controlled .

Mechanical properties of a biomaterial implant for bone should closely match that of the replaced or reinforced tissue. In the event of compliance mismatch, there could be loosening of the implant resulting in irritation of the surrounding tissue and the formation of a fibrous capsule around the implant. This will prevent the formation of new blood vessels and will cause implant failure due to poor tissue integration. Compressive strength of human cortical bone ranges between 90 and 209 MPa and that of cancellous bone lies between 1.5 and 45 MPa. Previous mechanical compressive strength of CPEGMC when hydrated ranged between 8-28 KPa [44]. In our study we incorporated different concentrations of HA to PEGMC to make CPEGMC/HA (30), CPEGMC/HA (45) and CPEGMC/HA (60) composites. The hydrated and non hydrated composites achieved $\sim 100\%$ recovery when compressed to 50% strain. The compressive modulus for hydrated and non hydrated CPEGMC/HA (30) and CPEGMC/HA (45) were comparable. Increasing concentration of HA resulted in an increase in the compressive modulus. Repeated cyclic compressive tests to study the ability of the composites to withstand repeated loading and unloading showed that the fully hydrated constructs were elastic showing 100% recovery with very negligible

hysteresis. Thus the addition of HA improved the mechanical strength of PEGMC without compromising the inherent elastic properties of the PEGMC.

The implanted biomaterial must be biodegradable. Furthermore the rate of degradation must closely match the rate of tissue regeneration. Presence of ester bonds in the PEGMC backbone as confirmed by FT-IR renders the CPEGMC/HA composites biodegradable. The degradation study showed that lower HA concentration in the polymer network results in faster degradation. This suggests that the polymer itself is degrading but the HA matrix is slow to degrade. Degradation samples at all time points maintained their structural integrity and there was no significant leaching of HA.

Hydroxylapatite(HA) was added to the crosslinking mixture consisting of PEGMC, NaHCO_3 , PEG-DA 3400 and redox initiators APS/TEMED. HA has been widely used in bone related applications due to its similarity to the inorganic CaP found in natural bone [45]. The ability to induce mineralization resulting in better tissue integration is an important consideration of bone tissue engineering. The rate and extent of mineralization can be a directly related to the material's bioactivity [46]. CPEGMC/HA composite was crosslinked using different concentrations of HA. Even at concentration of CPEGMC/HA : 30/70, the crosslinking mixture was injectable and crosslinkable. In this study, addition of HA resulted in the surface of the CPEGMC/HA (45) films to be completely covered in CaP minerals when place in 5X SBF. CPEGMC films when incubated in the same solution however showed no such bioactivity.

High porosity in scaffolds is desirable for tissue engineering applications. Natural bone morphology consists of trabecular bone which has inherent porosity of 50-90%. Therefore porosity and pore size of scaffolds used in bone tissue engineering is an important consideration [47]. We found CPEGMC and its composites CPEGMC/HA

(30), CPEGMC/HA (45) and CPEGMC/HA (60) created a highly porous structure when fully hydrated with pore size in range of 100- 400 μm . Previous studies have shown a minimum pore size of 100 μm is necessary for cell infiltration in tissue engineering application. For bone applications, pore size of 300 μm is considered optimum to facilitate bone and capillary formation [47, 48].

In vitro cellular studies were conducted using hFOB 1.19 osteoblasts. Cellular surface seeding of osteoblasts on CPEGMC and CPEGMC/HA films showed poor cellular attachment. All the attached cells on the unmodified CPEGMC and CPEGMC/HA surface had a rounded morphology with minimal cellular spreading [38]. The films were modified by covalently immobilizing collagen on the surface. On modification of the surface, there was a significant improvement in osteoblast attachment. Modification of surface with collagen improves osteoblast attachment due to the presence of N-containing groups such as amine on the surface. A small number of these amine groups could be positively charged due to protonation in the culture media thereby providing preferable sites for attachment [49]. Collagen modified CPEGMC/HA films showed better cellular attachment compared to CPEGMC films. This confirms that HA promotes greater osteoblast attachment [39].

Cellular encapsulation in hydrogels has numerous advantages. Cells can be delivered easily in an injectable system to the desired site. As the hydrogel crosslinks in situ, the crosslinking solution can penetrate into the surrounding tissue resulting in better adhesion of the scaffold minus the glues and sutures. Also injectable system will result in ease of administration and avoid the difficulties in making scaffolds of different dimensions as the injectable solution will fill and crosslink according to the gap that exists. Considerations for designing a suitable hydrogel for cell encapsulation are many. The polymer should be water soluble. The crosslinking conditions must be mild and cytocompatible. On encapsulation, the hydrogel should allow enough room

for the cells to grow and also allow easy exchange of media and other nutrients. The rate of degradation of the hydrogel should match the rate of tissue regrowth. Hydrogels that are covalently crosslinked are more desirable as the mechanical, degradation, extent and time to crosslink can be better controlled [50]. We evaluated the suitability of osteoblast encapsulation in CPEGMC and CPEGMC/HA films. Fluorescent photomicrographs of encapsulated osteoblasts using LIVE/DEAD assay showed that osteoblast encapsulation in CPEGMC/HA showed greater cell number at day 21. Osteoblast viability was studied using DNA assay. Total DNA content reduced at day 14 but increased at day 21 for both CPEGMC and CPEGMC/HA films. Osteoblast activity in CPEGMC and CPEGMC/HA were evaluated by measuring the ALP activity and calcium content. ALP in the presence of HA was found to be greater at day 21 as compared to CPEGMC. ALP is considered an early marker for osteoblastic differentiation. ALP is an ectoenzyme, phosphatase that is associated with cell membrane which is considered an early indicator of osteoblast differentiation and early ECM mineralization. Calcium is a late osteogenic differentiation marker for osteoblast activity. ALP activity and calcium content increased on day 21 after reducing at day 14. The ALP and Calcium content was more prominent in the case of CPEGMC/HA [48, 51].

CHAPTER 5

CONCLUSION

We have developed a citric acid based injectable composite PEGMC/HA that can be crosslinked in situ with free radical initiators. The PEGMC was synthesized using simple polycondensation reaction. Addition of HA with suitable crosslinker and initiator resulted in the formation of CPEGMC/HA. These hydrogels composites had tunable mechanical properties and degradation profile. Collagen modification of surface improved cellular adhesion. Cellular encapsulation of hFOB 1.19 osteoblasts showed good viability and cellular activity as determined by ALP activity and calcium content. Thus, CPEGMC/HA can be evaluated as a minimally invasive in situ crosslinking biomaterial for bone tissue engineering.

CHAPTER 6

FUTURE RECOMMENDATIONS

- 1) In vivo study of the injectable polymer will help in evaluating if the injectable CPEGMC/HA composite can induce bone regeneration.
- 2) To achieve a long term release of DFO from the hydrogel and study the possible complementary effect on angiogenesis.
- 3) To study the mechanical properties of decellularized bone reinforced with CPEGMC/HA.

REFERENCES

- [1] D. Gyawali, R. Tran, K. Guleserian, L. Tang, and J. Yang, “Citric-acid-derived photo-cross-linked biodegradable elastomers.” *Journal of biomaterials science. Polymer edition*, 2010.
- [2] G. Bran, J. Stern-Straeter, K. Hormann, F. Riedel, and U. Goessler, “Apoptosis in bone for tissue engineering,” *Archives of medical research*, vol. 39, no. 5, pp. 467–482, 2008.
- [3] J. Dawson and R. Oreffo, “Bridging the regeneration gap: stem cells, biomaterials and clinical translation in bone tissue engineering,” *Archives of biochemistry and biophysics*, vol. 473, no. 2, pp. 124–131, 2008.
- [4] J. Kretlow and A. Mikos, “Review: mineralization of synthetic polymer scaffolds for bone tissue engineering,” *Tissue Engineering*, vol. 13, no. 5, pp. 927–938, 2007.
- [5] M. Kofron and C. Laurencin, “Bone tissue engineering by gene delivery,” *Advanced drug delivery reviews*, vol. 58, no. 4, pp. 555–576, 2006.
- [6] R. Langer and J. Vacanti, “Tissue engineering,” *Science*, vol. 260, pp. 920–926, 1993.
- [7] L. Freed, G. Vunjak-Novakovic, R. Biron, D. Eagles, D. Lesnoy, S. Barlow, and R. Langer, “Biodegradable polymer scaffolds for tissue engineering,” *Nature Biotechnology*, vol. 12, no. 7, pp. 689–693, 1994.
- [8] D. Logeart-Avramoglou, F. Anagnostou, R. Bizios, and H. Petite, “Engineering bone: challenges and obstacles,” *Journal of Cellular and Molecular Medicine*, vol. 9, no. 1, pp. 72–84, 2005.

- [9] K. Rezwan, Q. Chen, J. Blaker, and A. Boccaccini, “Biodegradable and bioactive porous polymer/inorganic composite scaffolds for bone tissue engineering,” *Biomaterials*, vol. 27, no. 18, pp. 3413–3431, 2006.
- [10] K. Athanasiou, C. Zhu, D. Lanctot, C. Agrawal, and X. Wang, “Fundamentals of biomechanics in tissue engineering of bone.” *Tissue engineering*, vol. 6, no. 4, p. 361, 2000.
- [11] S. Weiner and H. Wagner, “The material bone: structure-mechanical function relations,” *Annual Review of Materials Science*, vol. 28, no. 1, pp. 271–298, 1998.
- [12] T. Branfoot, “Research directions for bone healing,” *Injury*, vol. 36, no. 3, pp. S51–S54, 2005.
- [13] J. Kanczler and R. Oreffo, “Osteogenesis and angiogenesis: the potential for engineering bone,” *Eur Cell Mater*, vol. 15, no. 2, pp. 100–114, 2008.
- [14] K. Burg, S. Porter, and J. Kellam, “Biomaterial developments for bone tissue engineering,” *Biomaterials*, vol. 21, no. 23, pp. 2347–2359, 2000.
- [15] P. Habibovic and K. de Groot, “Osteoinductive biomaterials-properties and relevance in bone repair,” *Journal of Tissue Engineering and Regenerative Medicine*, vol. 1, no. 1, pp. 25–32, 2007.
- [16] Q. Hu, B. Li, M. Wang, and J. Shen, “Preparation and characterization of biodegradable chitosan/hydroxyapatite nanocomposite rods via in situ hybridization: a potential material as internal fixation of bone fracture,” *Biomaterials*, vol. 25, no. 5, pp. 779–785, 2004.
- [17] W. Suchanek and M. Yoshimura, “Processing and properties of hydroxyapatite-based biomaterials for use as hard tissue replacement implants,” *Journal of Materials Research*, vol. 13, no. 1, pp. 94–117, 1998.

- [18] A. Di Martino, M. Sittinger, and M. Risbud, “Chitosan: a versatile biopolymer for orthopaedic tissue-engineering,” *Biomaterials*, vol. 26, no. 30, pp. 5983–5990, 2005.
- [19] W. Hennink and C. Van Nostrum, “Novel crosslinking methods to design hydrogels,” *Advanced Drug Delivery Reviews*, vol. 54, no. 1, pp. 13–36, 2002.
- [20] R. Payne, M. Yaszemski, A. Yasko, and A. Mikos, “Development of an injectable, in situ crosslinkable, degradable polymeric carrier for osteogenic cell populations. part 1. encapsulation of marrow stromal osteoblasts in surface crosslinked gelatin microparticles,” *Biomaterials*, vol. 23, no. 22, pp. 4359–4371, 2002.
- [21] R. Stile and K. Healy, “Thermo-responsive peptide-modified hydrogels for tissue regeneration,” *Biomacromolecules*, vol. 2, no. 1, pp. 185–194, 2001.
- [22] M. Lutolf and J. Hubbell, “Synthesis and physicochemical characterization of end-linked poly (ethylene glycol)-co-peptide hydrogels formed by michael-type addition,” *Biomacromolecules*, vol. 4, no. 3, pp. 713–722, 2003.
- [23] J. Temenoff and A. Mikos, “Injectable biodegradable materials for orthopedic tissue engineering,” *Biomaterials*, vol. 21, no. 23, pp. 2405–2412, 2000.
- [24] J. Kretlow, L. Klouda, and A. Mikos, “Injectable matrices and scaffolds for drug delivery in tissue engineering,” *Advanced drug delivery reviews*, vol. 59, no. 4-5, pp. 263–273, 2007.
- [25] J. Ifkovits and J. Burdick, “Review: Photopolymerizable and degradable biomaterials for tissue engineering applications,” *Tissue engineering*, vol. 13, no. 10, pp. 2369–2385, 2007.
- [26] R. Tran, Y. Zhang, D. Gyawali, and J. Yang, “Recent developments on citric acid derived biodegradable elastomers,” *Bone*, vol. 19, p. 25, 2010.

- [27] R. Tran, P. Thevenot, D. Gyawali, J. Chiao, L. Tang, and J. Yang, "Synthesis and characterization of a biodegradable elastomer featuring a dual crosslinking mechanism," *Soft Matter*, vol. 6, no. 11, pp. 2449–2461, 2010.
- [28] J. Yang, A. Webb, S. Pickerill, G. Hageman, and G. Ameer, "Synthesis and evaluation of poly (diol citrate) biodegradable elastomers," *Biomaterials*, vol. 27, no. 9, pp. 1889–1898, 2006.
- [29] J. Dey, H. Xu, J. Shen, P. Thevenot, S. Gondi, K. Nguyen, B. Sumerlin, L. Tang, and J. Yang, "Development of biodegradable crosslinked urethane-doped polyester elastomers," *Biomaterials*, vol. 29, no. 35, pp. 4637–4649, 2008.
- [30] X. Zheng Shu, Y. Liu, F. Palumbo, Y. Luo, and G. Prestwich, "In situ crosslinkable hyaluronan hydrogels for tissue engineering," *Biomaterials*, vol. 25, no. 7-8, pp. 1339–1348, 2004.
- [31] S. Jo, H. Shin, A. Shung, J. Fisher, and A. Mikos, "Synthesis and characterization of oligo (poly (ethylene glycol) fumarate) macromer," *Macromolecules*, vol. 34, no. 9, pp. 2839–2844, 2001.
- [32] J. Temenoff, H. Park, E. Jabbari, D. Conway, T. Sheffield, C. Ambrose, and A. Mikos, "Thermally cross-linked oligo (poly (ethylene glycol) fumarate) hydrogels support osteogenic differentiation of encapsulated marrow stromal cells in vitro," *Biomacromolecules*, vol. 5, no. 1, pp. 5–10, 2004.
- [33] S. Peter, M. Yaszemski, L. Suggs, R. Payne, R. Langer, W. Hayes, M. Unroe, L. Alemany, P. Engel, and A. Mikos, "Characterization of partially saturated poly (propylene fumarate) for orthopaedic application," *Journal of Biomaterials Science, Polymer Edition*, vol. 8, no. 11, pp. 893–904, 1997.
- [34] A. Oyane, H. Kim, T. Furuya, T. Kokubo, T. Miyazaki, and T. Nakamura, "Preparation and assessment of revised simulated body fluids," *Journal of Biomedical Materials Research Part A*, vol. 65, no. 2, pp. 188–195, 2003.

- [35] S. Kim, M. Park, S. Gwak, C. Choi, and B. Kim, "Accelerated bonelike apatite growth on porous polymer/ceramic composite scaffolds in vitro," *Tissue engineering*, vol. 12, no. 10, pp. 2997–3006, 2006.
- [36] C. Tas *et al.*, "Synthesis of biomimetic ca-hydroxyapatite powders at 37° c in synthetic body fluids," *Biomaterials*, vol. 21, no. 14, pp. 1429–1438, 2000.
- [37] D. Wang, C. Williams, F. Yang, N. Cher, H. Lee, and J. Elisseeff, "Bioresponsive phosphoester hydrogels for bone tissue engineering," *Tissue Engineering*, vol. 11, no. 1-2, pp. 201–213, 2005.
- [38] J. Burdick and K. Anseth, "Photoencapsulation of osteoblasts in injectable rgd-modified peg hydrogels for bone tissue engineering," *Biomaterials*, vol. 23, no. 22, pp. 4315–4323, 2002.
- [39] S. Kim, M. Sun Park, O. Jeon, C. Yong Choi, and B. Kim, "Poly (lactide-co-glycolide)/hydroxyapatite composite scaffolds for bone tissue engineering," *Biomaterials*, vol. 27, no. 8, pp. 1399–1409, 2006.
- [40] C. Wan, S. Gilbert, Y. Wang, X. Cao, X. Shen, G. Ramaswamy, K. Jacobsen, Z. Alaql, A. Eberhardt, L. Gerstenfeld, *et al.*, "Activation of the hypoxia-inducible factor-1 α pathway accelerates bone regeneration," *Proceedings of the National Academy of Sciences*, vol. 105, no. 2, p. 686, 2008.
- [41] E. Schlicher, N. Postma, J. Zuidema, H. Talsma, and W. Hennink, "Preparation and characterisation of poly (d, l-lactic-co-glycolic acid) microspheres containing desferrioxamine," *International Journal of Pharmaceutics*, vol. 153, no. 2, pp. 235–245, 1997.
- [42] J. Temenoff, H. Shin, D. Conway, P. Engel, and A. Mikos, "In vitro cytotoxicity of redox radical initiators for cross-linking of oligo (poly (ethylene glycol) fumarate) macromers," *Biomacromolecules*, vol. 4, no. 6, pp. 1605–1613, 2003.

- [43] H. Shin, J. Temenoff, and A. Mikos, “In vitro cytotoxicity of unsaturated oligo [poly (ethylene glycol) fumarate] macromers and their cross-linked hydrogels,” *Biomacromolecules*, vol. 4, no. 3, pp. 552–560, 2003.
- [44] E. Montufar, T. Traykova, C. Gil, I. Harr, A. Almirall, A. Aguirre, and M. Ginebra, “Foamed surfactant solution as a template for self-setting injectable hydroxyapatite scaffolds for bone regeneration,” *Acta Biomaterialia*, pp. 876–885, 2010.
- [45] M. Kikuchi, S. Itoh, S. Ichinose, K. Shinomiya, and J. Tanaka, “Self-organization mechanism in a bone-like hydroxyapatite/collagen nanocomposite synthesized in vitro and its biological reaction in vivo* 1,” *Biomaterials*, vol. 22, no. 13, pp. 1705–1711, 2001.
- [46] Y. Chou, W. Chiou, Y. Xu, J. Dunn, and B. Wu, “The effect of ph on the structural evolution of accelerated biomimetic apatite,” *Biomaterials*, vol. 25, no. 22, pp. 5323–5331, 2004.
- [47] M. Dadsetan, T. Hefferan, J. Szatkowski, P. Mishra, S. Macura, L. Lu, and M. Yaszemski, “Effect of hydrogel porosity on marrow stromal cell phenotypic expression,” *Biomaterials*, vol. 29, no. 14, pp. 2193–2202, 2008.
- [48] J. Wang, Y. Asou, I. Sekiya, S. Sotome, H. Orii, and K. Shinomiya, “Enhancement of tissue engineered bone formation by a low pressure system improving cell seeding and medium perfusion into a porous scaffold,” *Biomaterials*, vol. 27, no. 13, pp. 2738–2746, 2006.
- [49] Z. Cheng and S. Teoh, “Surface modification of ultra thin poly (-caprolactone) films using acrylic acid and collagen,” *Biomaterials*, vol. 25, no. 11, pp. 1991–2001, 2004.

- [50] G. Nicodemus and S. Bryant, “Cell encapsulation in biodegradable hydrogels for tissue engineering applications,” *Tissue Engineering Part B: Reviews*, vol. 14, no. 2, pp. 149–165, 2008.
- [51] J. Temenoff, H. Park, E. Jabbari, T. Sheffield, R. LeBaron, C. Ambrose, and A. Mikos, “In vitro osteogenic differentiation of marrow stromal cells encapsulated in biodegradable hydrogels,” *Journal of Biomedical Materials Research Part A*, vol. 70, no. 2, pp. 235–244, 2004.

BIOGRAPHICAL STATEMENT

Parvathi Nair was born in Trivandrum, India, in 1983. She received her Bachelor of Engineering degree from Pune University, India, in 2004 in Electronics and Telecommunication. She has worked as software engineer for close to three years, working in Capgemini India Pvt. Ltd, Mumbai, India from Feb 2007 to July 2008 before leaving to do her masters. After enrolling in the Biomedical Engineering program at the University of Texas at Arlington, she has been actively involved in developing and characterizing different biomaterials with a focus on bone tissue engineering. Her research interests include biomaterials and tissue engineering.